東海大學環境科學與工程研究所

碩士論文

改良磁性奈米銀觸媒進行異相催化臭氧去除水中腐植酸之研究

Modified Magnetic Silver nano-catalysts for Heterogeneous Catalytic Ozonation to Remove Humic acid in water

研究生：林世軒 撰

指導教授：張鎮南 博士

中華民國 101 年 7 月

東海大學碩士班研究生

論文指導教授推薦書

環境科學與工程學系林世軒君所提之論文

題目：改良磁性奈米銀觸媒進行異相催化臭氧去除水中腐植酸之研究

Modified Magnetic Silver Nano-Catalysts for Heterogeneous Catalytic Ozonation to Remove Humic acid in water

係由本人指導撰述，同意提付審查。

指導教授：張鎮南 （簽章）

101 年 7 月 13 日

東海大學環境科學系碩士班

論文口試委員審定書

環境科學與工程學系碩士班林世軒君所提之論文

題目：改良磁性奈米銀觸媒進行異相催化臭氧去除水中腐植酸之研究

Modified Magnetic Silver Nano-Catalysts for Heterogeneous Catalytic Ozonation to Remove Humic acid in water

---

經本委員會審議，認為符合碩士資格標準。

論文口試委員召集人 _____ (簽章)

委員 _____

_____

_____

中華民國 101 年 7 月 13 日

誌謝

首先誠摯的感謝指導教授張　鎮南博士的指導，老師的指導使我得以一窺環境工程領域的深奧，不時的討論並指點我正確的方向，使學生獲益匪淺。老師對學問的嚴謹更是我輩學習之典範。

本論文的完成另外亦得感謝宋孟浩　老師、馬英石　老師和陳谷汎　老師的支持及協助，老師們於百忙之中擔任學生的論文口試委員並給予指正和教導，使得本論文能夠更完整且嚴謹。

研究所兩年的生活，過得非常充實，感謝所上老師們的悉心教導以及系辦公室助理們的協助。並同時感謝實驗室的全體夥伴，慧燕學姊的幫助及勉勵，勳鍊、理維和煊根學長在實驗上的指導與幫忙，以及實驗室之花貴樺、伊婷和硯勛同學的共同砥礪，佑祺與志哲學弟與佳茹學妹的協助，也謝謝其他實驗室的同學們。你/妳們的陪伴讓兩年的研究生活變得絢麗多彩，使我永遠珍惜這份美好回憶。

最後謹以此文獻給我摯愛的家人，堅毅與病魔奮鬥的母親給予我勤奮不懈的動力。我能於碩士班獲取些微榮譽皆都源於母親的關懷及支持，同時也要感謝父親及三位姊姊的體諒和鼓勵，代替身為獨子的我照顧母親起居。因為有家人做為我最強大的後盾，我才能朝向目標前進，謝謝、謝謝。

摘要

本研究使用改良之磁性銀奈米顆粒 ($Fe_3O_4/SiO_2/Ag$) 進行異相催化臭氧化去除水中之腐植酸，並在系統中添加氫氧自由基捕捉劑以探討催化臭氧化之機制。已知 coumarin 與氫氧自由基反應後會形成中間產物 7-hydroxycoumarin，藉由中間產物的生成可以用以表示系統中氫氧自由基的存在。結果顯示，$Fe_3O_4/SiO_2/Ag$ 結合臭氧之中間產物產量高於單獨臭氧化系統，這是因為 $Fe_3O_4/SiO_2/Ag$ 能分解臭氧產生更多的氫氧自由基。而加入另一種氫氧自由基捕捉劑 TBA 後，可以觀察到中間產物的產量會因為氫氧自由基被捕捉而降低，而 $Fe_3O_4/SiO_2/Ag$ 結合臭氧之中間產物產量仍高於單獨臭氧化。結果顯示 $Fe_3O_4/SiO_2/Ag$ 結合臭氧增加了系統中氫氧自由基的含量。以 $Fe_3O_4/SiO_2/Ag$ 結合臭氧去除水中腐殖酸，只有在水溶液為酸性時，催化臭氧之效果會優於於單獨臭氧化，這是由於水溶液在高 pH 值時，臭氧之自解反應抑制了催化劑的效果。而以一階反應式之 K_d 值比較各式催化臭氧化之臭氧分解能力，發現本研究使用之催化臭氧化之 K_d 值為 $7.0\times10^{-4}\ s^{-1}$ 是單獨臭氧化 K_d 值之 1.75 倍。經由實驗證實 $Fe_3O_4/SiO_2/Ag$ 結合臭氧可以提升系統之氧化力並增加腐殖酸之去除率。

關鍵字：磁性顆粒、異相催化臭氧化、腐植酸、氫氧自由基、捕捉劑、coumarin、7-hydroxycoumarin、TBA

Abstract

This study used modified magnetic silver nanoparticles ($Fe_3O_4/SiO_2/Ag$) for the heterogeneous catalytic ozonation to remove humic acid (HA) in water. While hydroxyl radical (• OH) scavengers were added to the system in order to investigate the catalytic ozonation mechanisms. Coumarin is known to react with • OH to generate intermediate (7-hydroxycoumarin). The formation of the intermediate can be used to indicate the presence of • OH in the system. Compared to ozonation alone, $Fe_3O_4/SiO_2/Ag$ combined with ozone to produce more intermediate. This is due to the decomposition of ozone to produce more • OH by $Fe_3O_4/SiO_2/Ag$. Added another • OH scavengers of TBA can be observed production of intermediate will be reduced because the • OH was captured, while the intermediate produced in $Fe_3O_4/SiO_2/Ag$ combined with ozone is still higher than the ozonation alone. The results showed that $Fe_3O_4/SiO_2/Ag$ combined with ozone to improve the content of • OH in the system. To remove of humic acid by $Fe_3O_4/SiO_2/Ag$ combined with ozone, the humic acid removal rate is only higher than ozonation alone in acidic condition, this is due to the ozone self-decomposition inhibits the effect of the catalyst at high pH cases. Comparison of first-order ozone decay rate constants, the K_d values of this study of 7.0×10^{-4} s^{-1} and is 1.75 times than that of ozonation alone. The results indicated the presence of $Fe_3O_4/SiO_2/Ag$ could improve the oxidizing power of overall system and leading to the HA removal rate increased.

Keywords: magnetic particles, catalytic ozonation, humic acid, hydroxyl radicals, scavengers, coumarin, 7-hydroxycoumarin, TBA

CONTENTS

Table List

Figures List

Nomenclature

•OH	Hydroxyl Radicals	氫氧自由基
σ	Standard deviation	標準差
A·	Organic radical species	有機自由基物質
AC	Activated Carbon	活性碳
AH	Organic acid	有機酸
AOP	Advanced Oxidation Processes	高級氧化程序
COU	Coumarin	香豆素
CNT	Carbon nanotube	奈米碳管
DBP	Disinfection By Products	消毒副產物
DOC	Dissolved Organic Carbon	溶解性有機碳
EDS	Energy Dispersive Spectrometer	能量散佈分析儀
FA	Fulvic Acid	黃酸
HA	Humic Acid	腐植酸
HAA	Haloaceticacids	鹵化乙酸
HAAFP	Haloacetic Acid Formation Potential	鹵化乙酸生成潛能
HAN	Haloacetonitrile	鹵乙晴
Hc	Coercive force	抗磁力, 矯頑(磁)力
HPI	Hydrophilic	親水性

HPLC	High Performance Liquid Chromatography	高效液相層析儀
HPO	Hydrophobic	疏水性
HR-SEM	High Resolution Scanning Electron Microscope	高解析掃描式電子顯微鏡
HSs	Humic Substances	腐植質
K_d	First-order removal rate constant	一階反應去除率常數
K_1^{int}	Ionisation constants	電離常數
K_2^{int}	Ionisation constants	電離常數
Me_{red}	Reduced catalyst	還原態催化劑
$Me_{red}A^{\cdot}$	Organic radical species on reduced catalyst	還原態催化劑上之有機自由物質
MWCNT	Multi-Walled Carbon Nanotubes	多壁奈米碳管
Mr	Residual magnetization	殘留磁化強度
Ms	Saturation magnetization	飽和磁化強度
NOM	Natural Organic Matter	天然有機物質
NP_S	Nanoparticles	奈米顆粒
NSC	National Science Council	國家科學委員會
O_3	Ozone	臭氧
ORP	Oxidation Reduction Potential	氧化還原電位

P	Scavenger of hydroxyl radicals	氫氧自由基捕捉劑
P	Adsorbed primary by-products	吸附的初級副產物
P′	Primary by-products in solution	溶液中初級副產物
pKa	Acid dissociation constant	酸離解常數
R	Adsorbed final by-products	吸附的最終副產物
R′	Final by-products in solution	溶液中最終副產物
S	Catalyst surface	催化劑表面
SPIONs	Superparamagnetic Iron Oxide Nanoparticles	超順磁性鐵離子奈米顆粒
SQUID	Superconducting Quantum Interference Device	超導量子干涉磁量儀
SUVA	Specific UV Absorbance	比紫外光吸收值
TBA	Tert-Butyl Alcohol	第三丁醇
TEM	Transmission Electron Micrograph	電子顯微鏡
THM	Trihalomethanes	三鹵甲烷
THMFP	Trihalomethane Formation Potential	三鹵甲烷生成潛能
TOC	Total Organic Carbon	總有機碳
TPI	Transphilic	嗜水性
US	Ultrasonic	超聲波
UV	Ultraviolet	紫外光

UV_{254}	Ultraviolet wavelength of 254nm	254nm 波長之紫外光

Chapter 1 Introduction

1.1 Study Background

Water treatment has been regarded as an important international issue, because the water quality and processing costs will affect people's health and economic. Therefore, development of water recycling and renewable technologies is necessary.

Natural organic matters (NOMs) are complex organic compounds, the presence of NOMs in drinking water has been indicated that resulting the difficulty of drinking water treatment. So far, over 600 kinds of compounds were found in the drinking water disinfection processes. Especially Trihalomethanes (THM) and haloaceticacids (HAA) are the most common chemicals. The present process of disinfection (chlorine, ozone, chlorine dioxide, chloramines, and ultraviolet radiation) has been shown to produce different disinfection by products (DBPs) in water. Humic acid is the major component of NOMs, so it is also considered the formation of the main precursors of DBPs (Matilainen *et al.*, 2011).

Traditional disinfection processes were divided into physical, chemical and biological treatment. Selection of the processes according to the requirements of the water quality. In the case of high water quality requirements, the above three kinds of processes used in combination. For example, chemical oxidation can be effective mineralization of raw water, but usually combined with biological treatment to reduce the cost of processing. Therefore, advanced oxidation processes (AOPs) technology is continuously being developed for those intractable target pollutants, especially organic matters (Oller *et al.*, 2011).

AOPs technology is the use of highly active hydroxyl radicals (• OH) in oxidation process. Present technology includes Fenton, photo-Fenton, wet oxidation, ozonation, photocatalysis, etc. and their difference is the process of formation of free radicals (Kim and Ihm, 2011).

AOPs can be broadly divided into two types, the first type is Homogeneous reaction, and the second type, Heterogeneous reaction (Nawrocki and Hordern, 2010). In this study, the use of heterogeneous catalytic ozonation to remove NOMs in water. Heterogeneous catalytic ozonation is the use of solid catalysts for decomposition of ozone to the formation of more active • OH. Because ozone is difficult to complete mineralization of organic matter, heterogeneous catalytic ozonation is considered an effective method to reduce the DBPs.

The solid catalyst used in catalytic ozonation include Activated carbon (AC), carbon nanotube (CNT), metal oxides (e.g. MnO_2, TiO_2 or Al_2O_3), and the modification of metal oxide coated on the support (e.g. Cu-Al_2O_3 and Cu-TiO_2, Ru-CeO_2, VO/TiO_2, VO/silica gel, TiO_2/Al_2O_3 or Fe_2O_3/Al_2O_3). Among all, modified magnetic particles because of the easy of recovery and separation have been used for catalytic ozonation in recent years.

The existence of the highly active • OH were used as indicators of the catalytic ozonation reaction, however, due to the lifetime of • OH (10^{-9}s) is too short to directly measure the concentration of it. Although the direct measurement of • OH has been developed, such as electron paramagnetic resonance technique, but this method requires expensive equipment and high operating costs (Maezono *et al.*, 2011). Therefore, the use of the Hydroxyl radical scavengers to investigate the mechanism of catalytic ozonation were used in many studies. Hydroxyl radical scavengers were able to capture • OH

in catalytic ozonation, due to the specific reaction between scavengers and • OH. Coumarin and TBA were used in this study to differentiate between radical and non-radical mechanisms.

1.2 Objectives

The objectives of this study:

1. Synthesis of magnetic metal nanoparticle catalyst.
2. Investigate the mechanisms of catalytic ozonation and the effect of • OH.
3. Degrade natural organic matters.

Chapter 2 Literature Review

2.1 Natural organic matters

Natural organic matters (NOMs) are composed of several different compounds, most of which are aromatic and aliphatic. Because its composition is complicated, therefore, it is necessary to use the resin extracted and classified as hydrophilic (HPI) or hydrophobic (HPO) (Table 2-1) (Matilainen *et al.*, 2011). In addition, there is another extraction method which can classify the natural organic substances into three major portions (Zularisam *et al.*, 2011):

1. HPO or operationally defined as humic fraction with mainly carboxylic and phenolic functional groups (humic acids and fulvic acids).
2. Transphilic fraction (TPI), which has lower aliphatic/aromatic carbon contents than the HPO.
3. HPI or non-humic fraction corresponding to bases (primary and secondary protein groups), acids (amino acids), and neutral HPI (polysaccharide groups)(Fig. 2-1).

Table 2-1. Proposed composition of NOMs fractions separated using fraction techniques (Matilainen *et al.*, 2011).

Fraction	Organic compound class
Humic acid	Portion of humic substances precipitated at pH 1.
Hydrophobic acid	Soil fulvic acids, C_5 – C_9 aliphatic carboxylic acids, 1- and 2-ring aromatic carboxylic acids, 1- and 2- ring phenols
Hydrophobic base	1- and 2-ring aromatics (except pyridine), proteinaceous substances.
Hydrophobic neutral	Mixture of hydrocarbons, > C_5 aliphatic alcohols, amides, aldehydes, ketones, esters, > C_9 aliphatic carboxylic acids and amines, > 3 ring aromatic carboxylic acids and amines.
Hydrophilic acid	Mixtures of hydroxy acids, < C_5 aliphatic carboxylic acids, polyfunctional carboxylic acids.
Hydrophilic base	Pyridine, amphoteric proteinaceous material (i.e. aliphatic amino acids, amino sugars, < C_9 aliphatic amines, peptides and proteins).
Hydrophilic neutral	< C5 aliphatic alcohols, polyfunctional alcohols, short-chain aliphatic amines, amides, aldehydes, ketones, esters, cyclic amides, polysaccharides and carbohydrates.

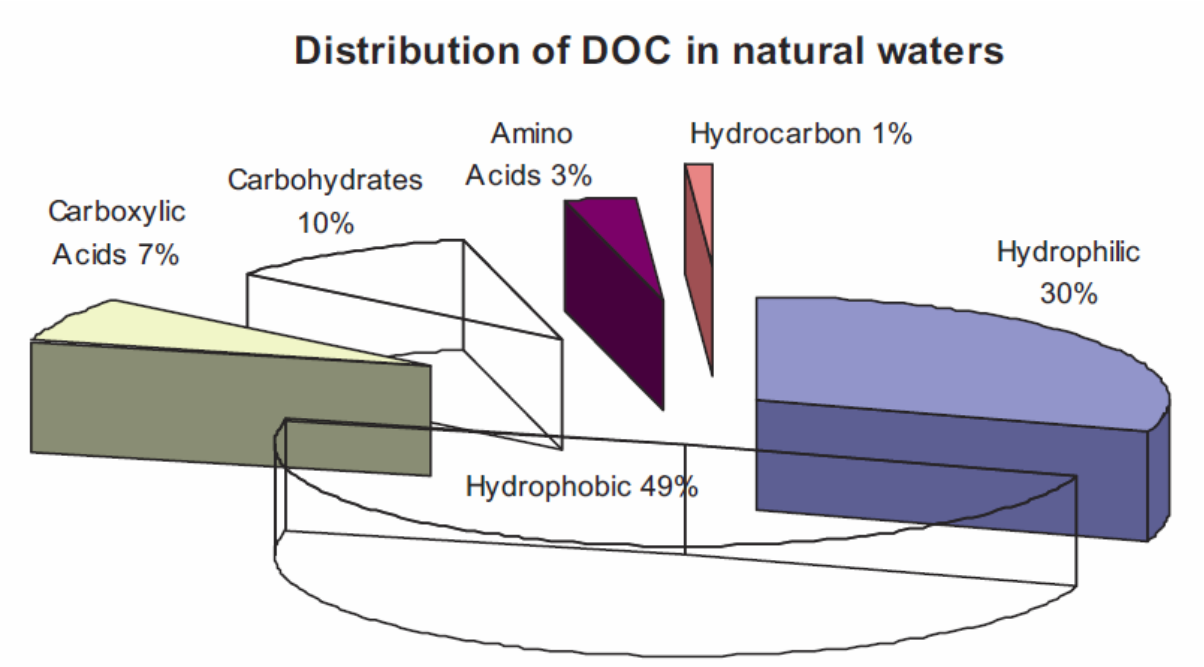

Fig. 2-1. Composition of NOM fraction in surface water based on DOC, sampling from UK (Zularisam *et al.*, 2011).

2.1.1 Humic substances

Humic substances (HSs) are the major part of NOMs, which are formed by the microbial degradation of animal and plant remains (such as plant tissue (litter) and animal excrement, fur and the corpses, etc.). They are difficult to be biodegradable, due to its complex molecular structure. The composition of HSs are different from each other based on the sources of water or soil, however, the average composition are similar. HSs can be operationally divided into three fractions based on their solubility in aqueous solutions as a function of pH. Humic acid (HA) is the fraction soluble in an alkaline solution, fulvic acid (FA) is the fraction soluble in an aqueous solution regardless of pH, and humin is the fraction insoluble at any pH value (Badis *et al.*, 2010).

2.1.2 The impact of natural organic matters on the environment

The presence of natural organic matters (NOMs) in drinking water has been confirmed that caused serious influence in the process. These problems include: (1) the negative impact on water quality, such as color, smell and taste, (2) makes the doses of coagulant and disinfectant demand increase, which led to the generation of sludge and harmful disinfection by-products (DBPs), (3) promote the growth of biological in disinfection system, and (4) improve the level of heavy metals and organic pollutants be adsorbed (Parilti *et al.*, 2011).

2.1.3 The quantified of natural organic matters.

NOM could quantified by measuring UV_{254}, Total organic carbon (TOC) concentrations, and dissolved organic carbon (DOC) concentrations (Chowdhury and Champagne, 2008). Roccaro and Vagliasindi (2009) reported that specific UV absorbance (SUVA) which can be used as a surrogate parameter to monitor the changes in aromatic nature of NOM in water was calculated from UV_{254} and DOC.

Chowdhury and Champagne (2008) noted the correlation between NOMs and THMs formation for the four water sources in Newfoundland (Fig. 2-2). Strong correlations between UV_{254} and THMs were found in all sources, with coefficients of determination (r^2) ranging between 0.77-0.92.

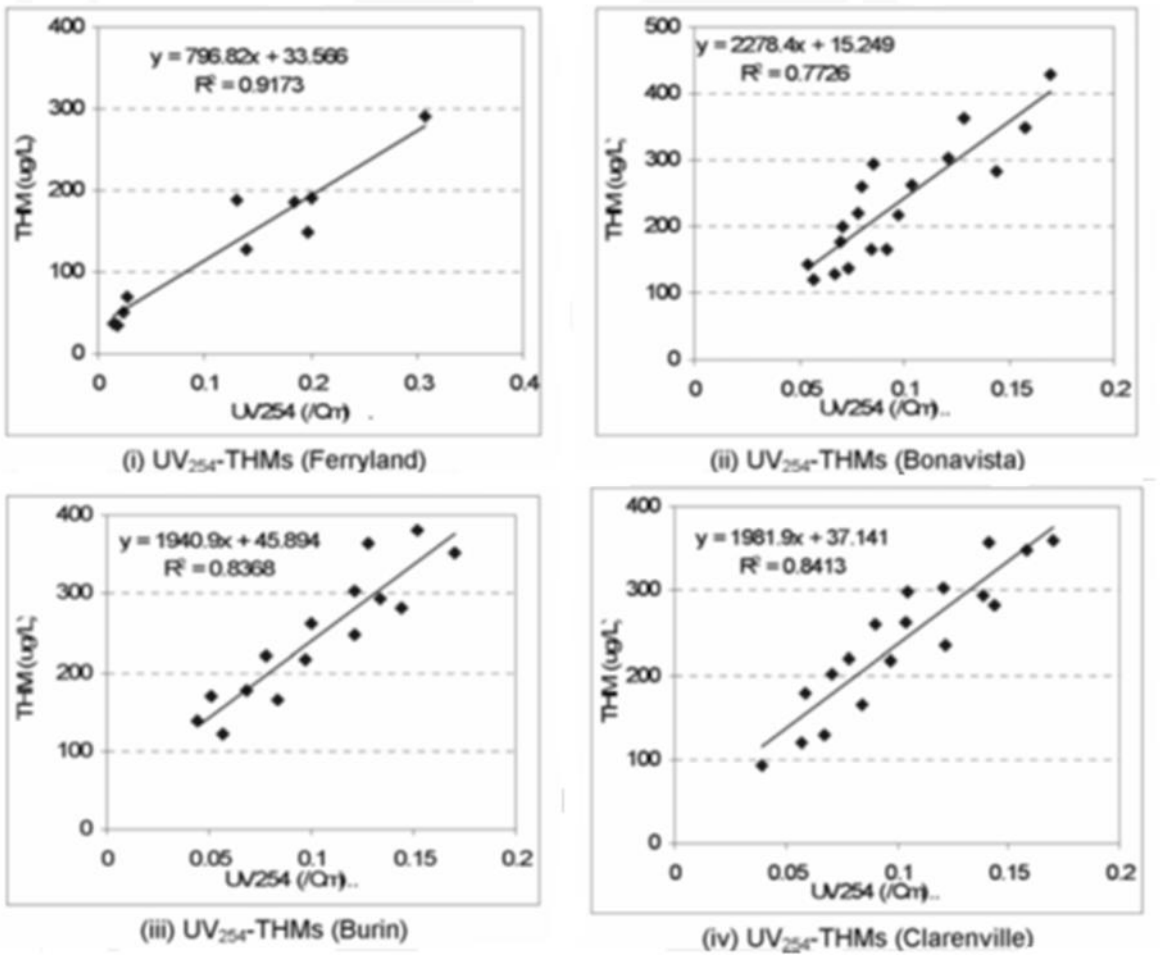

Fig. 2-2. Effects of UV_{254} on THMs formation, sampling form Canada (Chowdhury and Champagne, 2008).

2.2 Disinfection by products

The disinfectants commonly used in drinking water treatment include: chlorine, chlorine dioxide, chloramines and ozone. While chlorine is the most widely used, because of low cost, excellent bactericidal capacity and persistent disinfection. However, although the disinfection process to ensure the safety of drinking water, but it has also been confirmed that, these disinfectants may interact with dissolved organic matter to produce of DBPs. During the disinfection process, soluble organic substances could be converted to harmful DBPs including trihalomethanes (THMs), haloacetic acids (HAAs) and haloacetonitriles (HANs) (Liu *et al.*, 2011；Zhao et al., 2009). Humic acid is the main component of dissolved organic matter, was regarded as a precursor of DBPs (especially THMs). In order to reduce the formation of DBPs, researchers began developing a variety of removal of humic acid methods. Nevertheless, because of the stability of the molecular structure of humic acid, it is difficult to be completely degradation (mineralization), therefore recently the use of AOPs to remove humic acid, has obtained high attention.

2.3 Advanced Oxidation Processes (AOPs)

AOPs used in drinking water treatment can remove NOMs and reduce the formation of DBPs. Through generation of • OH in the reaction process, the pollutants may be degraded or mineralized into carbon dioxide and water. Previous studies have focused on ozone (O_3), ultraviolet radiation (UV) and hydrogen peroxide (H_2O_2), or used in combination (H_2O_2/UV；UV/O_3；H_2O_2/O_3) to get better removal. The classification of AOPs is shown in Table 2-2.

Table 2-2. The classification of advanced oxidation processes. Adapt from Kasprzyk-Hordern *et al.*(2003)

Reaction classification	Advanced oxidation processes
Homogeneous systems without irradiation	O_3/H_2O_2, O_3/OH^-, H_2O_2/Fe^{2+} (Fenton's reagent)
Homogeneous systems with irradiation	O_3/UV, H_2O_2/UV, O_3/H_2O_2/UV, photo-Fenton, electron beam, ultrasound, vacuum-UV
Heterogeneous systems with irradiation	TiO_2/O_2/UV
Heterogeneous systems without irradiation	electro-Fenton.

Lamsal *et al.,* (2011) proposed in that the total trihalomethane formation potential (THMFP) and haloacetic acid formation potential (HAAFP) are the major DBPs of the raw and oxidized waters (Fig. 2-3). Among all process, O_3, H_2O/O_3, H_2O_2/UV and O_3/UV have significant reduction in THMFP, while H_2O_2/UV and O_3/UV have good performance on decomposing of HAAFP. In general, (1) THMFP removal was greater than HAAFP in the oxidation processes, (2) H_2O_2/UV is the most effective, (3) The common point of these methods is the use of the formation of • OH in the oxidation as a strong

oxidant used to transform NOMs.

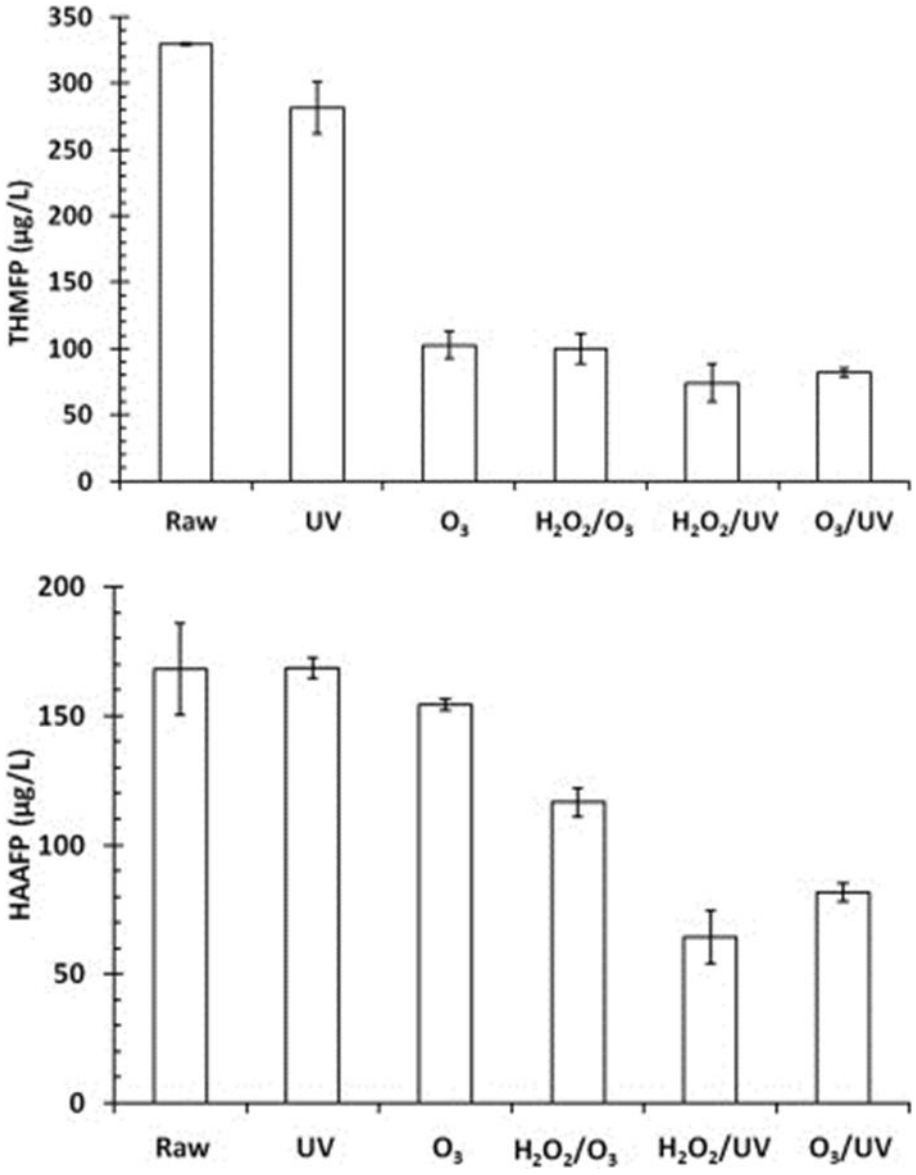

Fig. 2-3. THMs and HAAs for raw and oxidized waters (Vertical bars represent 2σ levels)(Lamsal *et al.*, 2011).

2.3.1 Ozone and Hydroxyl radicals

The electronic structure of the O_3 explains its high reactivity, while O_3 molecule represents a hybrid, formed by the two possible resonance structures (Fig. 2-4.). Van Geluwe *et al.* (2011) indicated that the positive formal charges on the central oxygen atom in both resonance structures explains the electrophilic character of O_3. Conversely, the excess negative charge present in one of the terminal atoms imparts a nucleophilic character to O_3. These properties make O_3 an extremely reactive compound. The vast abundance of unsaturated bonds in humic substances facilitates the efficient decomposition of these compounds by O_3. The unsaturated bonds in these molecules are transformed to oxygenated saturated bonds. This is schematically represented in Fig. 2-5., where a model structure of a humic acid molecule is drawn, before and after O_3 oxidation.

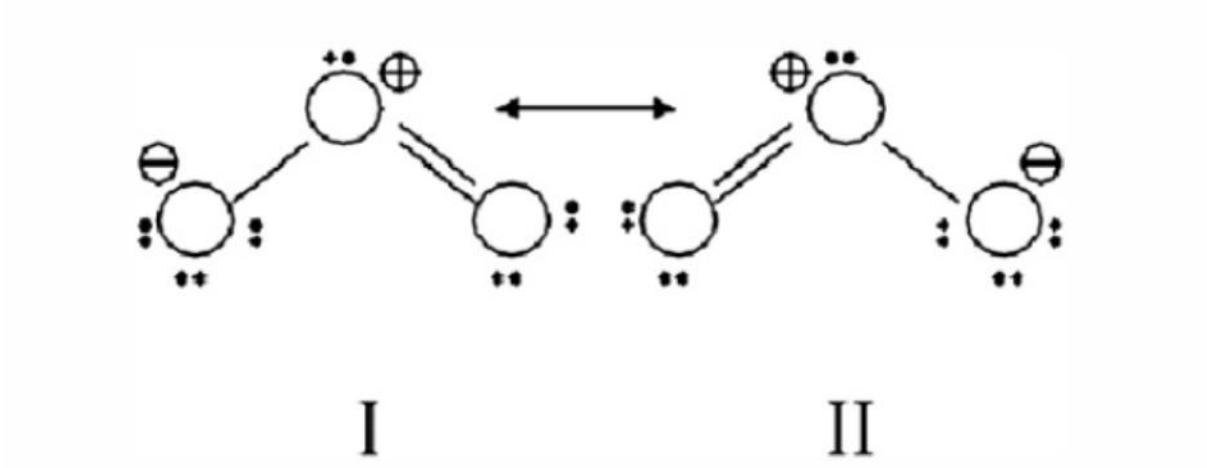

Fig. 2-4. Resonance forms of the O_3 molecule (Van Geluwe *et al.*, 2011).

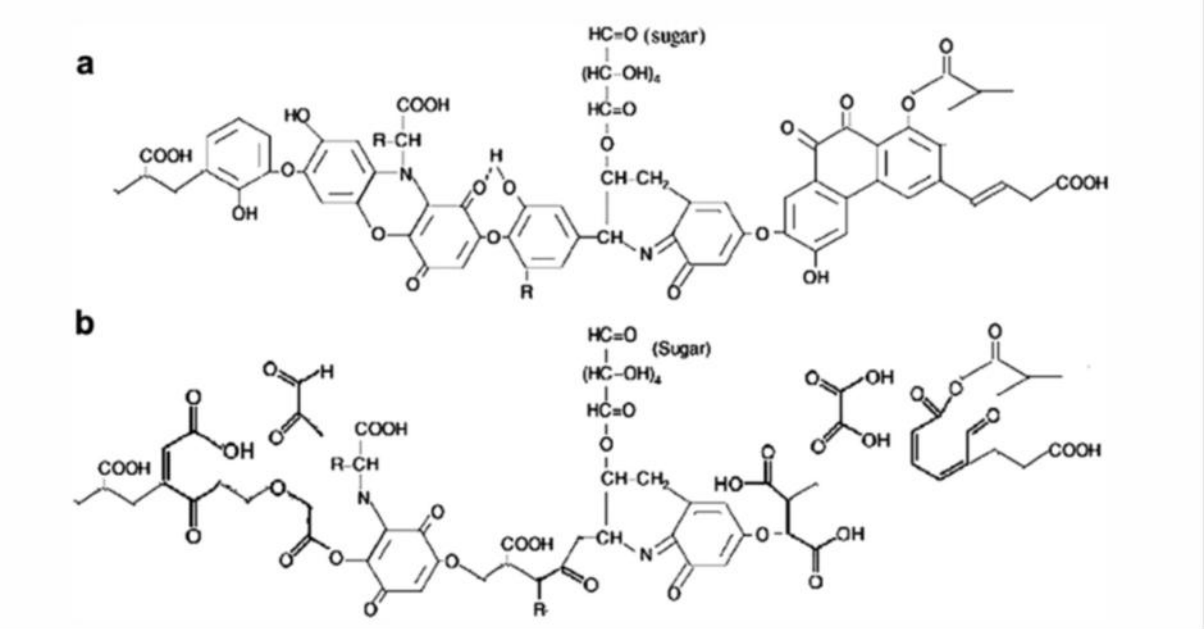

Fig. 2-5. A hypothetical structure of humic substances (a) before and (b) after O_3 oxidation (Song *et al.*, 2004).

Ozonation is divided into direct and indirect reactions, the direct reaction of ozone molecules directly react with dissolved substances, while the indirect reaction is the use of free radicals formed in the ozone decomposition. Compared with the ozone, • OH is a non-selective oxidant, because its standard reduction potential (2.80V) (Eq. 1) is higher than the ozone (2.07V) in the ozone oxidation process (Eq. 2) (Pillai *et al.*, 2009). Due to its high reactivity, • OH can react with almost all types of organics (ethylenic, lipid, aromatic, aliphatic) and inorganics (anions and cations), while the indirect reaction of ozone on the removal of natural organic matter is more favorable (Van Geluwe *et al.*, 2011).

$O_3 + 2H^+ + 2e^- \leftrightarrows O_2 + H_2O$ (E^0 = 2.07 V (SHE))..... (1)

$^{\bullet}OH + H^+ + e^- \leftrightarrows H_2O$ (E^0 = 2.80 V (SHE))..... (2)

Staehelin and Hoigne´ (1985) reported the decomposition of O_3 in water is a radical-type chain reaction, where various solutes can act as initiators, promoters or inhibitors .

Initiation step: The decomposition of O_3 is initiated by OH ions (Eq. 3), and this leads to the formation of one superoxide anion ($^{\bullet}O_2^-$) and one hydroperoxyl radical ($^{\bullet}HO_2$), which are in an acid-base equilibrium ($pK_a = 4.8$):

$$O_3 + OH^- \rightarrow {}^{\bullet}O_2^- + {}^{\bullet}HO_2 \ (k= 70\ M^{-1}S^{-1}) \quad \text{.....(3)}$$

In addition, the reaction of unsaturated bonds in NOM with O_3 can lead to the consumption of O_3 (Eq. 4), or the production of an ozonide ion radical ($^{\bullet}O_3^-$) by an electron transfer reaction (Eq. 5):

$$O_3 + NOM \rightarrow NOM_{OX.} \quad \text{.....(4)}$$

$$O_3 + NOM \rightarrow NOM^+ + {}^{\bullet}O_3^- \quad \text{.....(5)}$$

Propagation step: $^{\bullet}O_2^-$ is a highly selective catalyst for the decomposition of O_3 in water. The rate constant with which $^{\bullet}O_2^-$ reacts with O_3 molecules is very high and results in the formation of $^{\bullet}O_3^-$:

$$^{\bullet}O_2^- + O_3 \rightarrow {}^{\bullet}O_3^- \quad (k = 1.6\times10^9\ M^{-1}S^{-1}) \quad \text{.....(6)}$$

$$^{\bullet}O_3^- + H+ \rightarrow {}^{\bullet}HO_3 \quad (k= 5\times10^{10}\ M^{-1}S^{-1}) \quad \text{.....(7)}$$

$$^{\bullet}HO_3 \rightarrow {}^{\bullet}OH + O_2 \quad (k= 1.4\times10^5\ M^{-1}S^{-1}) \quad \text{.....(8)}$$

The decomposition of O_3 in pure water is well-described in the Staehelin and Hoigne´ model, which is widely used for predicting the lifetime of O_3 in natural waters (Van Geluwe *et al.*, 2011). This model is shown in Fig. 2-6.

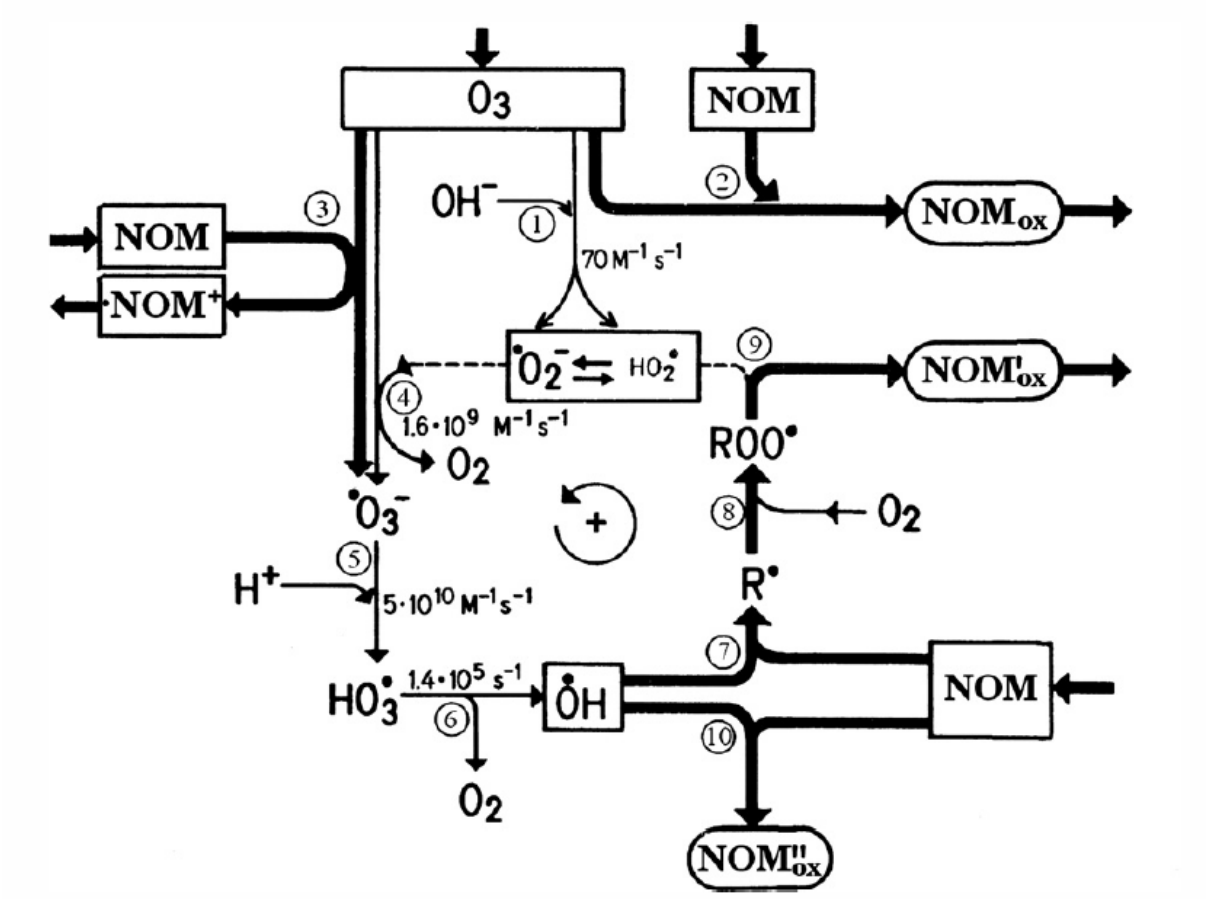

Fig. 2-6. Reactions of aqueous O_3 in the presence of NOM, which reacts with O_3 or with OH radicals (scavenging or converting ˙OH into ˙HO_2) (Staehelin and Hoigne´, 1985).

2.3.2 Hydroxyl radicals scavengers

Because the reaction may generate free radicals as a specific intermediate, therefore the radicals scavengers were used as the capture of free radicals. In this case, coumarin could be used as a probe molecule as it is known to react with • OH leading to the formation of fluorescent 7-hydroxycoumarin (Ikhlaq *et al.*, 2012) (Fig. 2-7). Another scavengers also can be used to inhibit the reaction of • OH in the system through the high reaction rate with • OH. In this case, TBA reacts with • OH with a rate constant of $6\times10^{8}\,M^{-1}S^{-1}$, it is twice than that of TBA with ozone reaction ($3\times10^{8}\,M^{-1}S^{-1}$) (Hoigne´ and Bader, 1983).

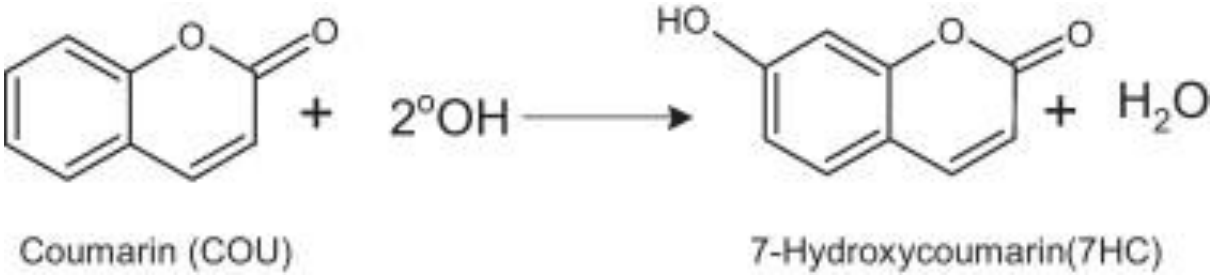

Fig. 2-7. Formation of 7-hydroxycoumarin (7-HC) in the reaction of coumarin (COU) with hydroxyl radicals (Ikhlaq *et al.*, 2012).

2.4 Catalytic ozonation

Ozone is a selective oxidant, it preferentially attacks molecules containing unsaturated bonds, leading to the formation of saturated compounds such as aldehydes, ketones and carboxylic acids. Due to their low reactivity towards ozone, these compounds tend to accumulate in water (Gonçalves *et al.*, 2012). To improve this situation, many studies have focused on how to increase the indirect reaction of the ozonation, that is, how to increase the decomposition of ozone to form • OH. Previously on catalytic ozonation research, including multi-walled carbon nanotubes (MWCNT), activated carbon (AC), metal ions, metal oxide, metal oxide on support, zeolite, ultrasonic (US), ultraviolet (UV), etc. (Li *et al.*, 2010; Guzman-Perez *et al.*, 2011; Liu *et al.*, 2011; Wang *et al.*, 2011; Mahmoodi *et al.*, 2011).

Kasprzyk-Hordern *et al.*(2003) proposed that catalytic ozonation can be considered firstly as homogeneous catalytic ozonation, which is based on ozone activation by metal ions present in aqueous solution, and secondly as heterogeneous catalytic ozonation in the presence of metal oxides or metals/metal oxides on supports. Catalytic ozonation was found to be effective for the removal of several organic compounds from drinking water and wastewater.

2.5 Homogeneous catalytic ozonation

Homogeneous catalytic ozonation is the use of transition metals in react ion with ozone, the solution pH and concentration of metal ions will determine the efficiency of the reaction. In general, it can be divided into two principal mechanisms (Kasprzyk-Hordern *et al.*, 2003):

1. The decomposition of ozone to form • OH s through the metal ion.

2. The oxidation of organic compounds with the catalyst.

In previous study had confirmed as an effective catalyst metal ions, including: Fe(II), Fe(III), Mn(II), Ni(II), Co(II), Cd(II), Cu(II), Ag(I),Cr(III), Cr(III), Zn(II) etc. Among the most widely used are: Mn(II), Fe(III), Fe(II), Co(II), Cu(II), Zn(II) and Cr(III) , and Fe(II)/O_3 and Fe(II)/O_3/UV processes are based on Fenton or photo-Fenton reactions. The catalytic activity of Mn(II), Fe(II), Fe(III), Cr(III), Ag(I), Cu(II),Zn(II), Co(II) and Cd(II) sulphate in the process of humic substances ozonation in water. To compare the removal of total organic carbon (TOC), it is obtained that the effect of the ozonation alone only 33%, not enough to make the pollutants completely mineralized, and in the homogeneous catalytic ozonation system, Mn (II) (62%) and Ag (I) (61%) are the most effective, other metal ions slightly less efficient (Nawrocki and Kasprzyk-Hordern, 2010)..

2.6 Heterogeneous catalytic ozonation

Heterogeneous catalytic ozonation is adding solid catalyst to the catalytic ozonation, which can both to increasing the amount of ozone dissolved, but also enhance the ozone decomposition to produce more • OH. Physical and chemical properties of the solid catalyst will determine the efficiency of the catalyst. Physical properties include: surface area, density, pore volume, porosity, pore size distribution as well as mechanical, strength, purity and commercial availability. Chemical properties includes: chemical stability and especially the presence of active surface sites such as Lewis acid sites, which are responsible for catalytic reactions (Kasprzyk-Hordern *et al.*, 2003). The most widely used catalysts in heterogeneous catalytic ozonation include: metal oxides, metals on supports, zeolites, activated carbon, and carbon nanotube, or modification of the above catalyst.

In the entire mechanisms of heterogeneous catalytic ozonation, including the gas, liquid and solid phase transfer. The reaction on the catalyst surface determines the heterogeneous catalytic ozonation efficiency, gaseous ozone molecules and organic compounds are adsorbed on the catalyst surface, which explains the added catalyst making the increase in the amount of ozone dissolved. Adsorbed substances will occupy the surface of the catalyst, making the ozone and organic substances cannot contact with the solid catalyst, which is why the specific surface area will determine the effect of the catalyst (Nawrocki and Kasprzyk-Hordern, 2010).

2.6.1 Surface properties of catalyst

Kasprzyk-Hordern *et al.* (2003) indicated that the main parameter, which determines the catalytic properties of metal oxides, is acidity and basicity.

Hydroxyl groups are present on all metal oxides surfaces. However, the amount and the properties of the hydroxyls depend on the metal oxide. The hydroxyl groups formed at metal oxide surface behave as Brönsted acid sites. Lewis acids (electron pair acceptor) and Lewis bases (electron pair donor) are sites located on the metal cation and coordinatively unsaturated oxygen, respectively. Both Brönsted and Lewis acid sites are thought to be the catalytic centers of metal oxide.

Metal oxides have amphoteric ion exchange capacity, and ion exchange properties are based on the ability of surface hydroxyl groups to dissociate or to be protonated depending on the pH value of the solution.

$$M\text{-}OH + H^+ \leftrightarrows M\text{-}OH_2^+ , \quad K_1^{int} \quad (9)$$

$$M\text{-}OH + OH^- \leftrightarrows M\text{-}O^- + H_2O , \quad K_2^{int} \quad (10)$$

K_1^{int} and K_2^{int} are the ionisation constants, as H^+ and OH^- are the potential determining ions, the surface charge will depend on the excess of one type of charged site over the other and is a function of solution pH. The point of zero charge, which is the pH at which the net surface charge is zero depends.

$$pH_{PZC} = 0.5(pK_1^{int} + pK_2^{int}) \quad (11)$$

At pH < pK_1^{int} metal oxide will act as an anion exchanger while at pH > pK_2^{int} it will act as cation exchanger as presented in Fig. 2-8.

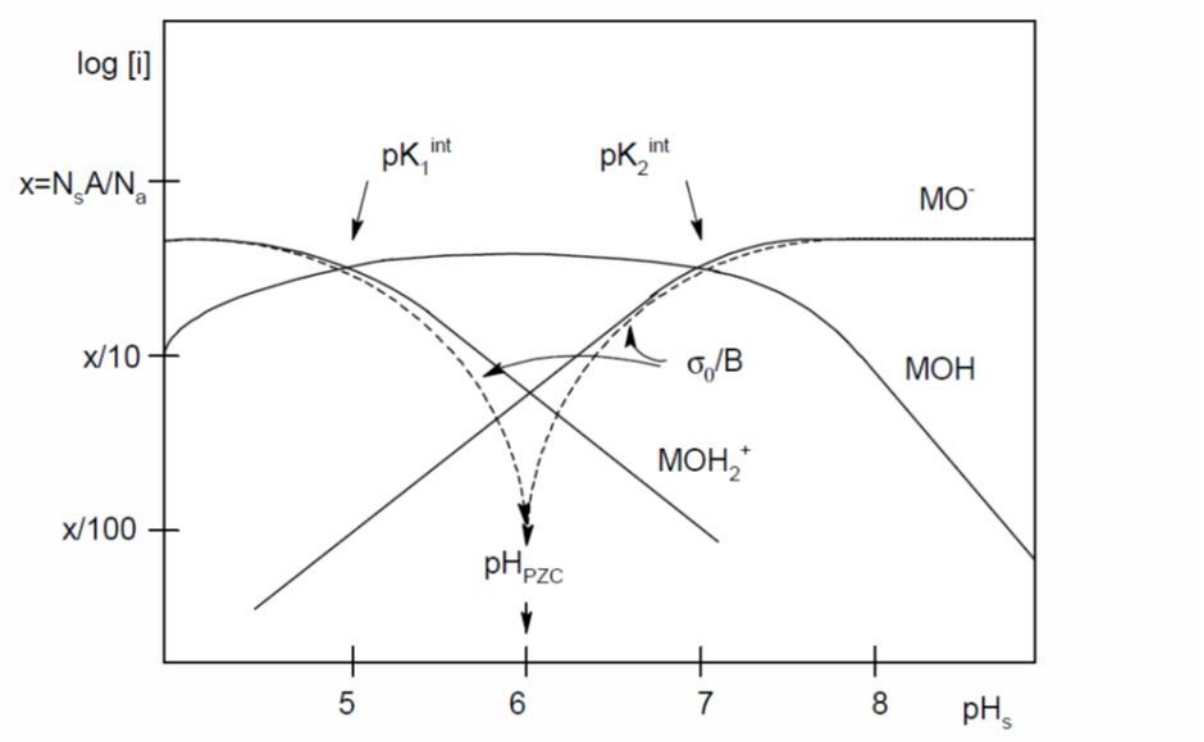

Fig. 2-8. Variation of charged and uncharged species concentration with the surface pH (pHs) (Kasprzyk-Hordern *et al.*, 2003).

2.6.2 Metal oxide and metal oxide on support

The study of solid catalyst on catalytic ozonation has focused on metal oxide or metal oxide on supports, Kasprzyk-Hordern *et al.*(2003) verified part of the metal oxide on the support of the ozone decomposition rate (Table 2-3). Its conclusion is the coated metal on the surface of the solid catalyst have higher ozone decomposition rate, the increase in the frequency of the electron transport and making the redox reaction increased. The catalytic activity order of metals supported on SiO_2 was found to be: Pd > Ag >Rh >Pt >Ni > Ru. Due to the low cost of Ag, it is considered to be economic catalytic metal. Nawrocki and Kasprzyk-Hordern (2010) indicated the application of both metal and support of catalysts in noble metals are efficient redox catalysts, which are able to decompose O_2 with the formation of oxygen-metal bound strong enough to provide effective ozone decomposition.

Table 2-3. The metal oxide on the support of the ozone decomposition rate. (adapted from Kasprzyk-Hordern *et al.*, 2003)

Metal	Al_2O_3	SiO_2	SiO_2-Al_2O_3	TiO_2
	Average rate (mg_{O3} min^{-1} $g^{-1}cat$)			
Ru	0.24	0.18	0.24	0.07
Rh	0.49	0.49	0.27	0.20
Pd	0.40	0.77	0.53	0.36
Ag	0.39	0.56	0.14	0.28
Ni	0.16	0.22	0.07	0.09
Pt	0.24	0.48	0.07	0.26

2.7 The mechanisms of catalytic ozonation.

Beltrán *et al.* (2002) reported the mechanisms of catalytic ozone decomposition proposed is as follows: (S is the catalyst surface, In the initiator of ozone decomposition, and P is the scavenger of • OH)

1. Homogeneous decomposition:

$O_3 + OH^- \rightarrow HO_2^- + O_2$ ..... (12)

$O_3 + HO_2^- \rightarrow HO_2^{\bullet} + O_3^{\bullet -}$ .....(13)

$O_3 + In \rightarrow O_3^{\bullet -} + In^+$ .....(14)

$HO_2^{\bullet} \leftrightarrows O_2^{\bullet -} + H^+$ ..... (15)

2. Heterogeneous decomposition surface reaction:

pH 2–6:

$O_3 + S \leftrightarrows O_3\text{-}S$ ..... (16)

$O_3\text{–}S \leftrightarrows O\text{-}S + O_2$ .....(17)

$O_3 + O\text{-}S \leftrightarrows 2O_2 + S$ .....(18)

pH > 6:

$OH^- + S \leftrightarrows OH\text{-}S$ .....(19)

$O_3 + OH\text{–}S \leftrightarrows {}^{\bullet}O_3\text{-}S + HO^{\bullet}$ .....(20)

${}^{\bullet}O_3\text{-}S \leftrightarrows {}^{\bullet}O\text{-}S + O_2$ .....(21)

$O_3 + {}^{\bullet}O\text{-}S \leftrightarrows O_2^{\bullet -} + S + O_2$ .....(22)

3. Homogeneous propagation and termination reactions:

$O_3 + O_2^- \rightarrow O_3^{\bullet -} + O_2$ ..... (23)

$O_3^{\bullet -} + H^+ \rightarrow HO_3^{\bullet}$ .....(24)

$HO_3^{\bullet} \rightarrow HO^{\bullet} + O_2$ ..... (25)

$HO_3^{\bullet} + P \rightarrow$ end products.....(26)

Legube and Karpel Vel Leitner (1999) proposed the mechanisms of catalytic ozonation (Fig. 2-9) and assume that there are two mechanisms occur between the catalyst and ozone.

Mechanism 1:

1. Catalyst as adsorbent only, no catalytic effect, and Ozone and • OH are the oxidant species.
2. Initial organic acid (AH,) would be quickly adsorbed on the support of catalyst.
3. Ozone (or • OH) would then oxidize the surface complex to give oxidation by-products either desorbed in solution (P' and R': primary and final by-products in solution, respectively,) or still adsorbed at the surface of catalyst (P and R: adsorbed primary and final by-products, respectively,).
4. The final adsorbed by-product (R) would desorb and thereafter be oxidized in homogeneous solution by ozone or • OH.

Mechanism 2:

1. The catalyst would react with both ozone and adsorbed organics.
2. Starting to the reduced catalyst (Me_{red}), ozone would oxidize metal.
3. Organic acids (AH) would be adsorbed on oxidized catalyst and then oxidized by an electron-transfer reaction to give again reduced catalyst ($Me_{red}A^{\bullet}$)
4. The organic radical species $A^{\bullet}$ would be then easily desorbed from catalyst and subsequently oxidized by OH or O_3 either in bulk solution, or more probably, into the thickness of electric double layer.

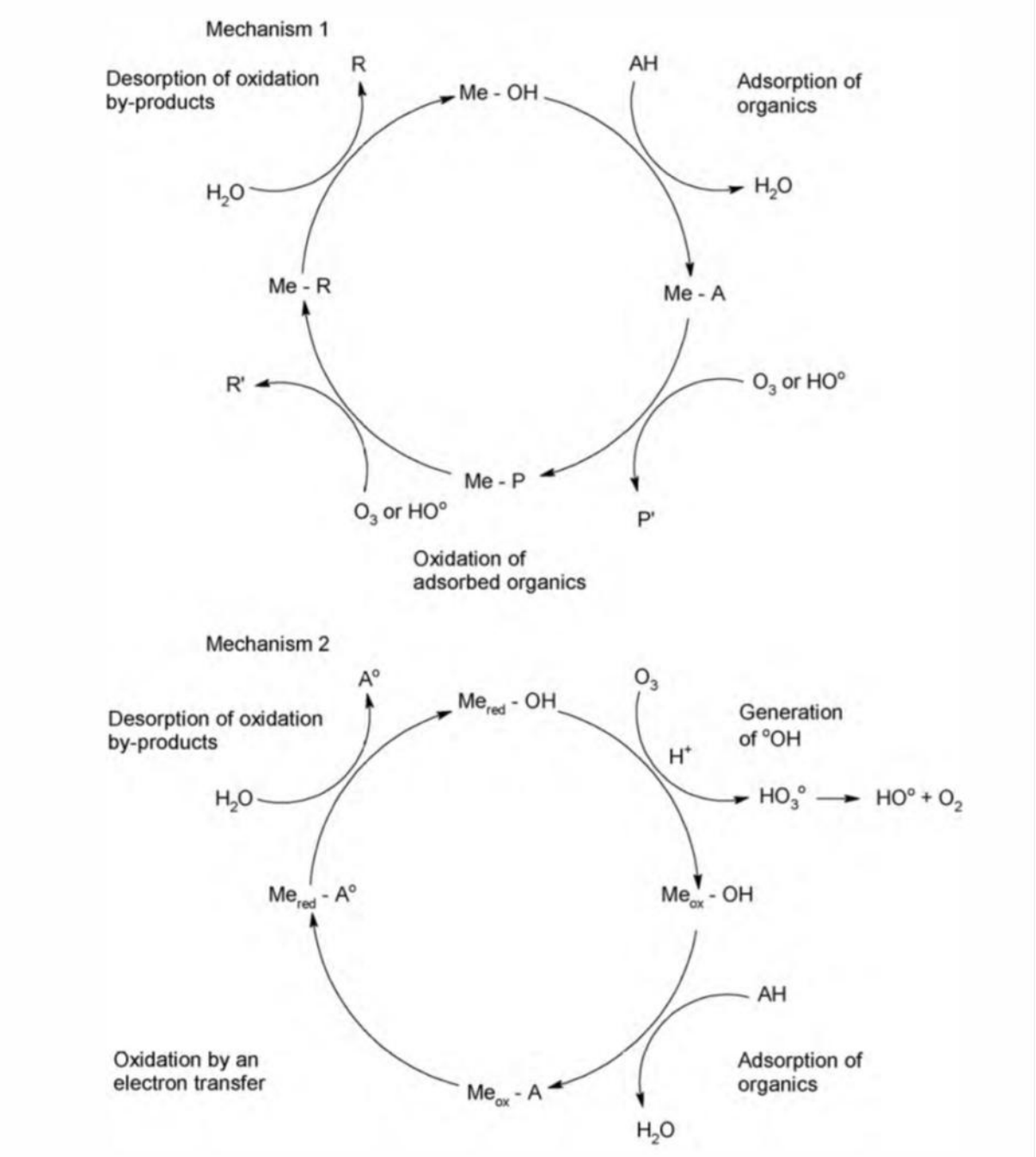

Fig. 2-9. Mechanisms of catalytic ozonation in the presence of metals on supports (AH - organic acid; P, R - adsorbed primary and final by-products; P′, R′ - primary and final by-products in solution respectively) (Nawrocki and Kasprzyk-Hordern, 2010).

2.8 Nanoparticles

Nanoparticles (NP_S) are solid and spherical structures ranging around 100 nm in size and prepared from natural or synthetic polymers. Within this range, the material of the nanostructures will have a completely different properties (compared to the original size) because of quantum effects. Due to the high specific area and high surface energy, NP_S is widely used in catalysts, biomedical (drug delivery, cell stain) and high-tech industries.

2.8.1 Superparamagnetic nanoparticles

The hysteresis curve (Fig. 2-10) was obtained by a Superconducting Quantum Interference Device (SQUID). Under constant temperature, demagnetized state; i.e., no extra magnetic field or induced magnetization; the magnetization will increase. The magnetization of catalyst particle will rise gradually with the magnetic field increasing from curve OABC till the saturation magnetization (Ms). While the magnetic field decreasing, the magnetic curve doesn't follow the original magnetization curve to the original point, instead, it dropping toward to the curve CD. This indicates the magnetization curve will reduce while the drop of magnetic field. When the magnetic field at zero (H=0) case, the magnetization curve doesn't back to the initial zero point, it implies a residual magnetization (Mr) occurred. The Mr phenomena can be defined as hysteresis.

The magnetization (saturation magnetization and coercive force) of magnetic particle may vary with the size, shape and structure of particle. When particle size reduce to a certain level, a superparamagnetic phenomenon will taking place. In this case, it will has no hysteresis affect and can be aggregated or recovered easily with the adoption of an excess magnetic field

(Lin, 2009). While the remove of excess magnetic field, the superparamagnetic particle will remain stable and stay with well dispersed condition.

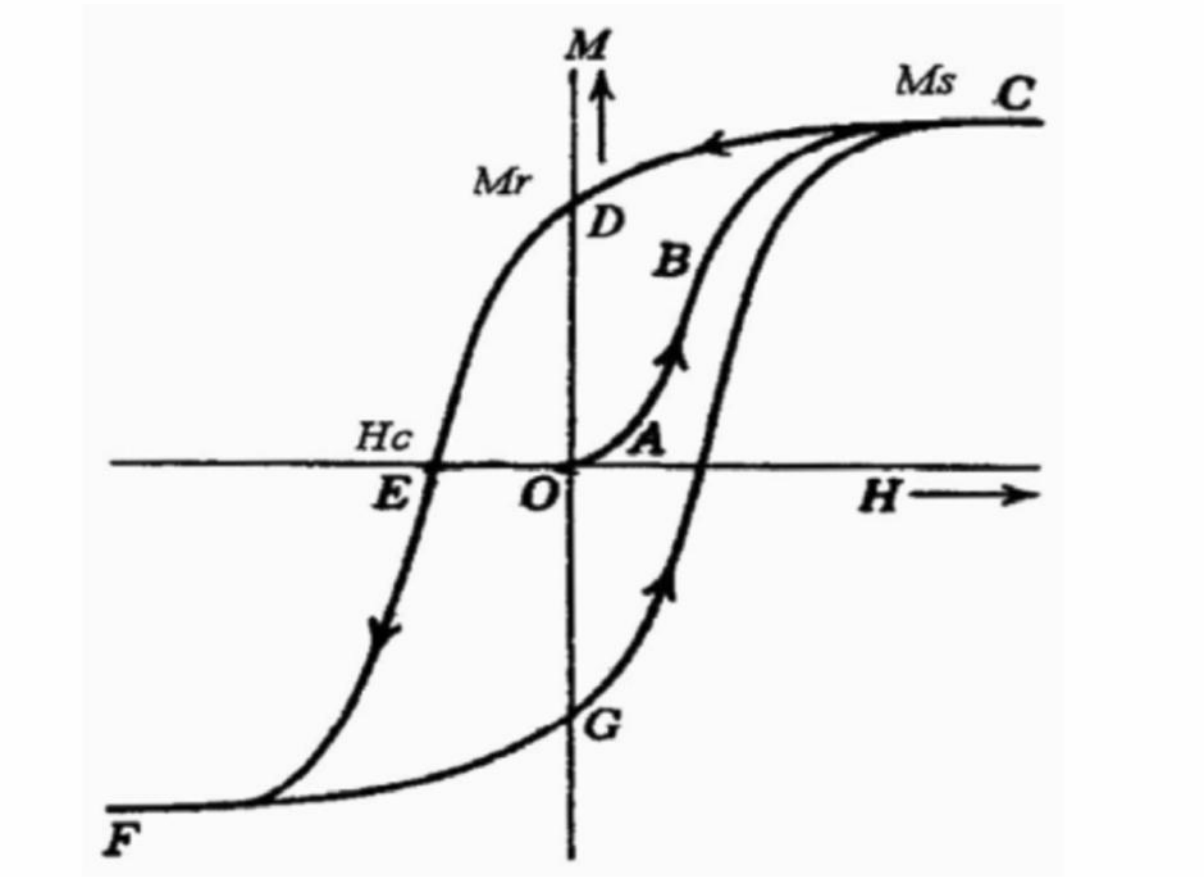

Fig. 2-10. The diagram of hysteresis (Ms – saturation magnetization; Mr – residual magnetization; Hc – coercive force) (Lin, 2009)

2.8.2 Metal magnetic nanoparticles

Due to their unique optical, electrical, magnetic and catalytic properties, metal nanoparticles have received much attention. Especially of noble metal particles in nanoscale (Au, Ag, Pt, etc.) have attracted intensive research interest due to their promising catalysis properties. However, because noble metal have high catalytic activity, meanwhile it also increased the cost of the catalyst, therefore, many studies of recovery methods on nobel metal have been proposed. The common filtering method in the recovery of nanoscale noble metal particles is difficult, and the filtration system will be contaminated by residual nanoparticles.

Depends on the development of magnetic materials, the use of magnetic recovery is considered to be high efficiency and low-cost method. The nobel metals particles can be coated on modified surface of magnetic material, and then recovery by the magnetic of particles. In addition to the ease of recycling, when the magnetic material presented the superparamagnetic state, but also can avoid the aggregation of particles and increasing the particle distribution in water (Pradeep and Anshup, 2009; Choi *et al.*, 2010).

Previous studies have reported several metals on the synthesis of magnetic metal particles. Both Lv *et al.*(2010) and Li *et al.* (2010) were reported a synthesis method about silver magnetic particles. Based on the Lv *et al.*(2010), the shape and product structure of nanoparticles can be observed by transmission electron micrograph (TEM) and shown in Fig. 2-11.

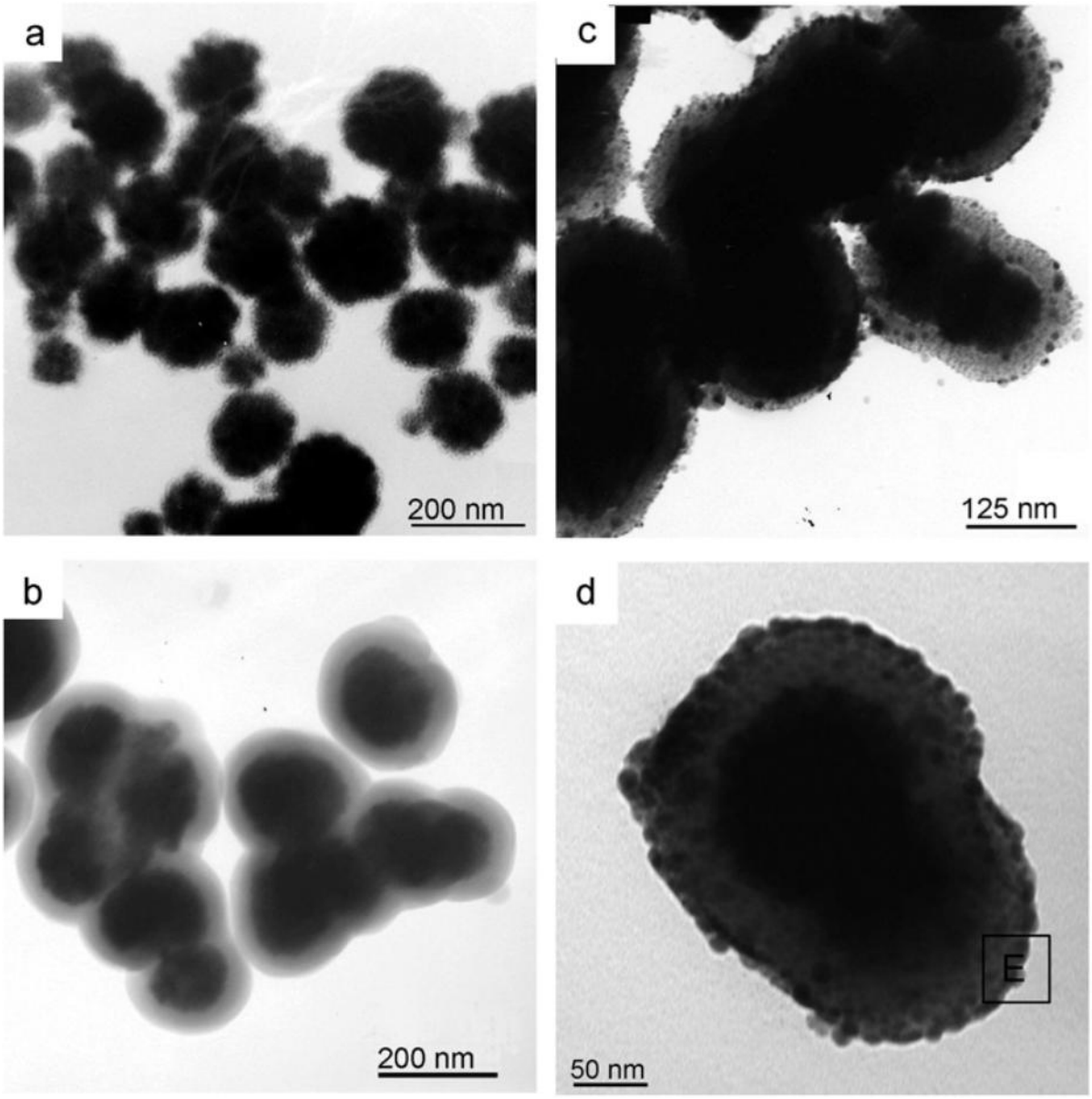

Fig. 2-11. TEM images of (a)Fe_3O_4, (b)Fe_3O_4\$SiO_2$, (c) and (d)$Fe_3O_4$\$SiO_2$\Ag (Lv *et al.*, 2010)

Chapter 3 Material and Methods

3.1 Experiment framework

In this study, the assembly of metal magnetic nanoparticles ($Fe_3O_4/SiO_2/Ag$) as catalyst was combined with ozonation to decompose humic acid in water. The purpose is using heterogeneous catalytic ozonation to removal NOMs and investigating the mechanism of AOPs. The Flow chart of this study is shown in Fig. 3-1.

Step 1. Synthesize noble metal magnetic nanoparticles as solid catalyst, and analyze the basic properties of the particles (magnetic hysteresis curve, the shape and product structure, crystal phase and the composition of the surface material).

Step 2. Conduct catalytic ozonation to decompose humic acid and investigate the reaction mechanisms. In order to achieve cost effective system, a recovery of the catalyst by analyses the reusability and change of basic properties was conducted.

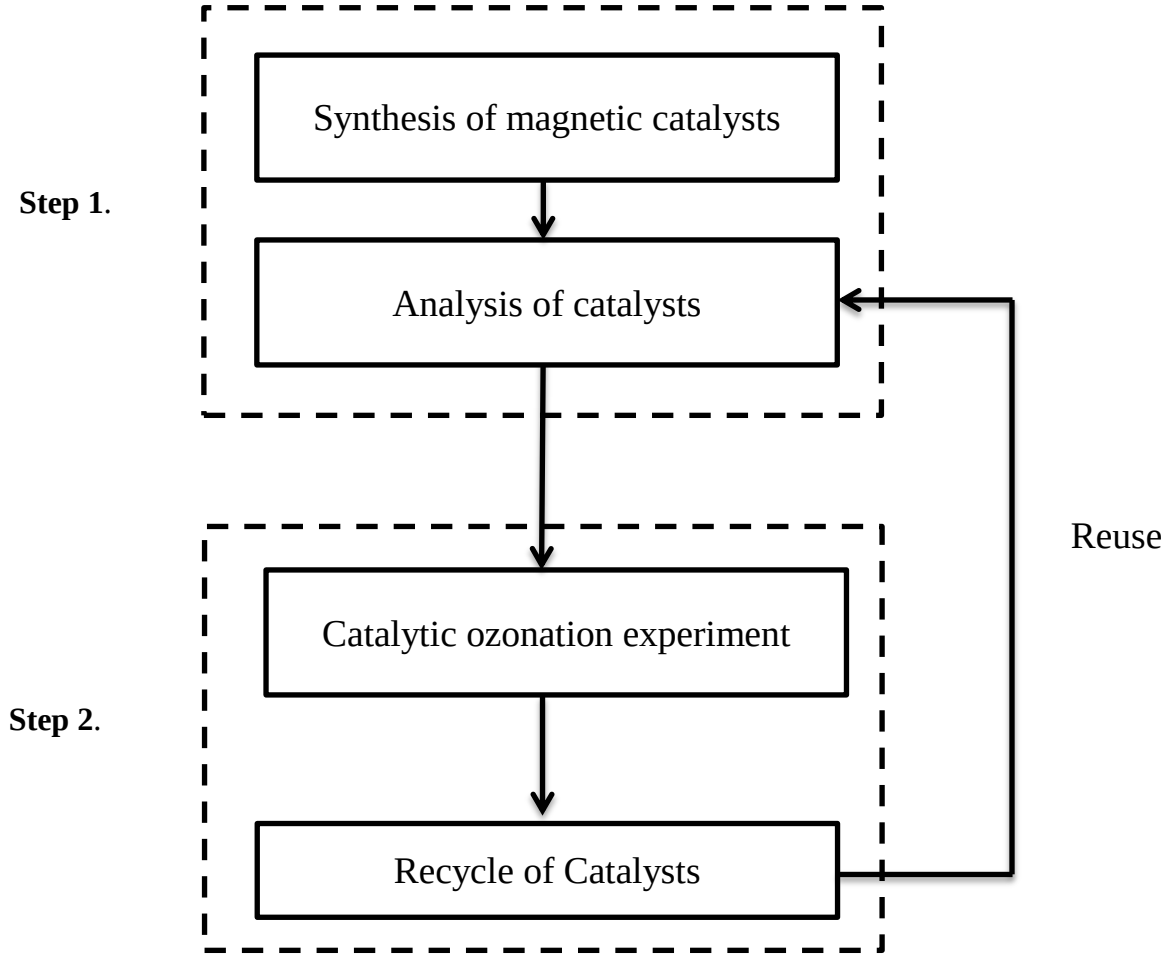

Fig. 3-1. The Flow chart of catalytic ozonation**.**

3.2 Preparation of commercial humic acid solution

This study adapted commercial humic acid dissolved in deionized water (in alkaline conditions, pH > 12), and then measured its content of DOC after membrane filtration (0.45 μm). Various initial concentrations of humic acid aqueous solution (5, 10 and 20 mg/L), were used in the overall tests.

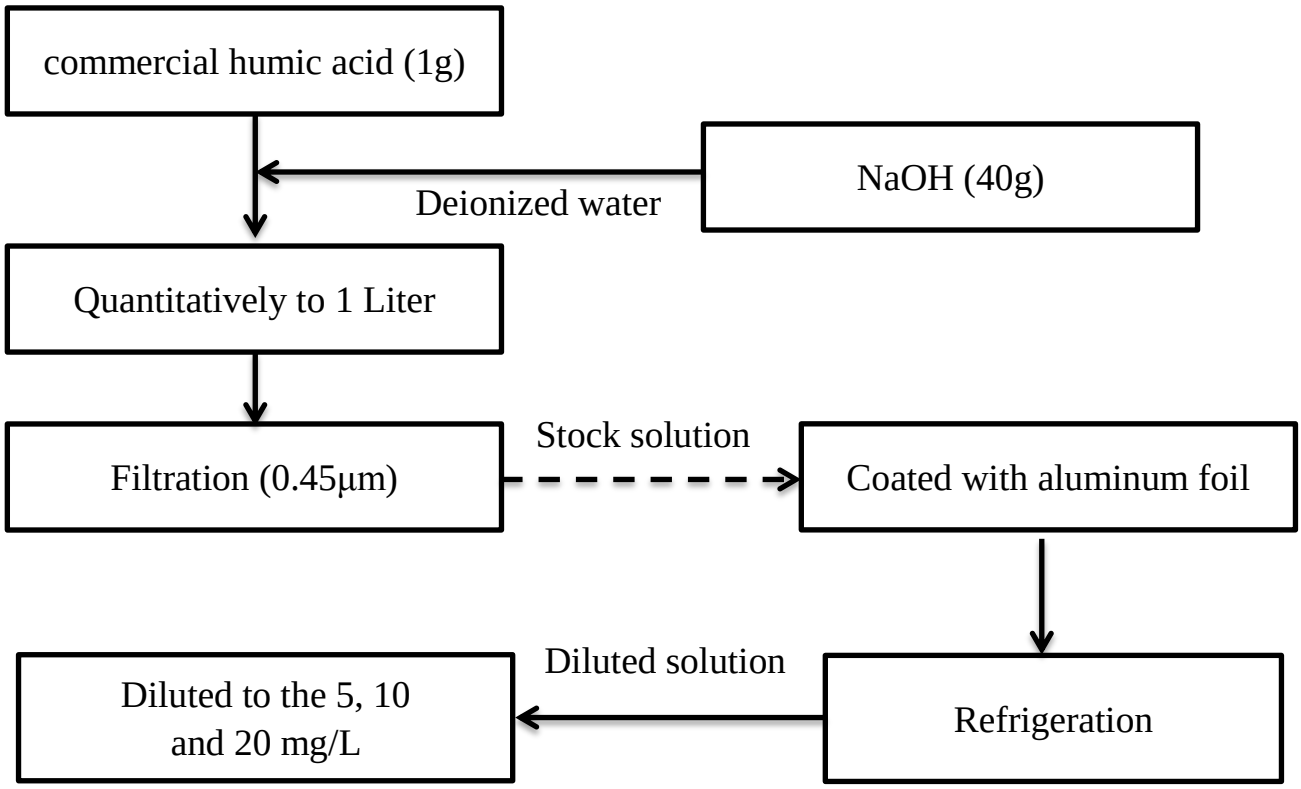

Fig. 3-2. The Flow chart of stock and diluted humic acid solution preparation.

Table 3-1 Reagents for preparation of commercial humic acid.

Reagent	Cas/Catalog number	Maker	Country
Sodium hydroxide (NaOH)	1310-73-2	Merck	Germany
Humic acid sodium salt	H1, 675-2	Aldrich	USA

3.3 The preparation of magnetic catalysts

3.3.1 Synthesis of Fe_3O_4 nanoparticles

In this study, the core of magnetic catalyst (Fe_3O_4 nanoparticles) was obtained by co-precipitation (Mahmoudi *et al.*, 2011). 2.54g of ferric chloride ($FeCl_2$*$4H_2O$) and 9.74g of ferrous chloride ($FeCl_3$) were added to 500 mL of deionized water. Then added ammonia hydroxide solution (NH_4OH) at 85°C. After that, the precipitate was washed three times with deionized water and dried at 105 ℃.

3.3.2 Preparation of Fe_3O_4/SiO_2 particles

Fe_3O_4/SiO_2 structures were prepared by sol-gel method which was proposed by Ghosh *et al.*, (2011). Added magnetic material (Fe_3O_4) into the mixed solution containing deionized water, ammonia (98 mL), and isopropanol (392 mL), then ultrasonicated for 30 min by ultrasonic cleaning bath. After that, tetraethyl orthosilicate (15-20 mL) was added to the solution slowly at 40°C and the solution was stirred (550 rpm) for 5 hours. The precipitate (Fe_3O_4/SiO_2) was separated by magnetic force and washed three times with deionized water.

3.3.3 Preparation of Fe_3O_4/SiO_2/Ag particles

The preparing electroless metal plating was following the methods proposed by Lv *et al.*, 2010 to coat silver on the surface of magnetic nanoparticles (Fe_3O_4/SiO_2) (equ. 30). Based upon Eq. 30, the 0.50 g of magnetic particles (Fe_3O_4/SiO_2) were dispersed in 50 mL mixture

solution of stannous chloride (0.60 g) and hydrochloride acid (10.92 mL) and the solution was ultrasonicated for 30 min. After ultrasonic, the particles were re-dispersed in 50 mL of ammonical silver nitrate aqueous solution and sonicated for 1h. Then, the precipitate ($Fe_3O_4/SiO_2/Ag$) was separated and dried at 60°C.

$$Sn^{2+} + 2[Ag(NH_3)_2]^{+} \rightarrow Sn^{4+} + 2Ag + 2NH_3 \quad (30)$$

Table 3-2. Regents and equipments for preparation of catalyst ($Fe_3O_4/SiO_2/Ag$).

Reagent	Cas/Catalog/HS number	Maker	Country
Ferric chloride ($FeCl_2*4H_2O$)	13478-10-9	Merck	Germany
Ferric chloride ($FeCl_3$)	7705-08-0	Merck	Germany
Ammonium hydroxide solution (NH_4OH)	2814-20-00	Merck	Germany
Isopropanol ($CH_3CHOHCH_3$)	67-63-0	Mallinckrodt	USA
Tetraethyl orthosilicate (TEOS)	78-10-4	Merck	Germany
Stannous chloride ($SnCl_2*2H_2O$)	10025-69-1	Merck	Germany
Silver nitrate ($AgNO_3$)	7761-88-8	Merck	Germany
Hydrochloric acid fuming 37% (HCl)	2806-10-00	Merck	Germany
Equipments	Model	Maker	Country
Ultrasonic cleaning bath	Power Sonic 420	Hwashin Technology	South Korea

3.4 The ozonation system

A 3 Liters semi-batch Pyrex glass reactor equipped with a 500 rpm mixer and three monitored sensors (pH, ORP and DO_3) were connected with rapid digital storage oscilloscope (Yokogawa, OR100E, Japan) were used in this study. The reaction temperature was maintained at 25 ± 2℃ by water bath (RCB 60, Taiwan). Ozone molecules generated with ozone generator (AirSep Corp., KA-1600, USA) by corona discharge. The flow rate of ozone stream was controlled by a mass-flow controller and continuously introducing into the reactor at a flow rate of $4{,}000 \pm 23$ mL/min.

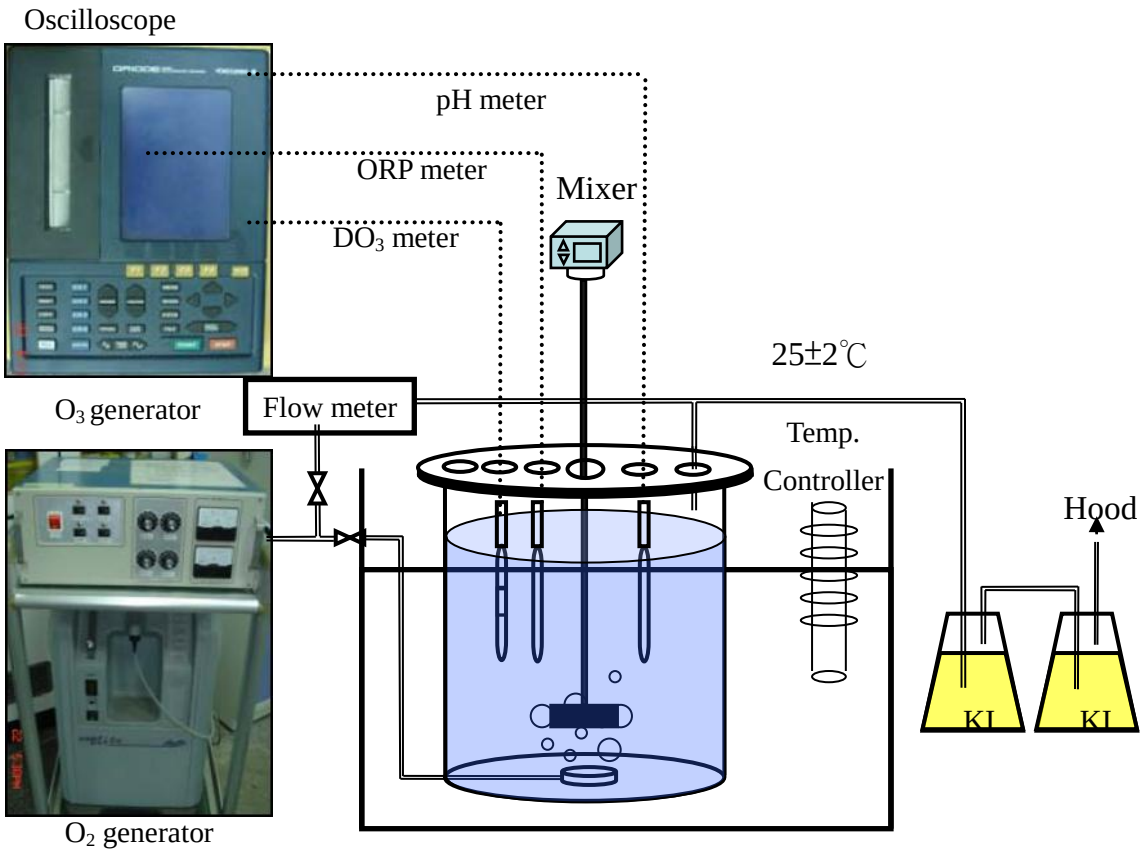

Fig. 3-3. Schematic diagrams of ozonation system (semi-batch Pyrex glass reactor, mixer, online monitored sensors (pH, ORP and DO_3), oscilloscope, water bath and O_3/O_2 generator)

Table 3-3. The equipment of ozonation system.

Equipment	Specification and Operation Conditions
Digital storage Oscilloscope (Yokogawa, OR100E, Japan)	Channel: Four channel Frequency: 60 MHz Scan rate: 1 Gs/S Data collected: 16,000 data storage per second
Water bath (RCB 60, Taiwan)	Temperature range: 4~100℃ Inner diameter: W350×D450×H500 mm Power: 220V, 60 Hz, 15A
Ozone generator (AirSep Corp., KA-1600, USA)	Flow rate: 5,000±41 mL/min Ozone production: 0-16 g/hr (Max) Ozone concentration: 10-60 g/m3 (Max) Oxygen demand: 2~12 L/min Outer diameter: W430×D410×H178 mm Power: 110 V, 60 Hz, 2.5 A
Nitrogen separator (oxygen generator) (AirSep Corp., KA-1600, USA)	Flow rate: 2~5 L/min Outer diameter: W380×D400×H710 mm Power: 110 V, 60 Hz, 4 A
Mixer (Shin kwang, DC-1S, Taiwan)	Rotationl Speed: 80~1,150 rpm Torque: 2.5 kg/cm Motor: 100 W Power: AC 110/220 V, 50/60 Hz

3.5 Analysis method

3.5.1 Analysis of catalyst

The properties of the catalyst (hysteresis curve, shape, structure, crystalline phase, surface composition and elemental analysis) were analyzed by the precision instrument (SQUID, TEM, SEM and EDS) of the National Science Council (NSC) in National Cheng Kung University. Zeta potential of particles was analyzed by the zeta potential and submicron particle size analyzers (Beckman Coulter Delsa™Nano C).

TABLE 3-4. Analysis instruments of the catalyst ($Fe_3O_4/SiO_2/Ag$).

Instrument	Function	Country
Superconducting Quantum Interference Device Vibrating Sample Magnetometer (SQUID VSM)	Hysteresis curve	USA
Transmission Electron Microscope (TEM, JEOL JEM-1400)	Shape and structure	Japan
High Resolution Scanning Electron Microscope and Energy Dispersive Spectrometer (HR-SEM and EDS, HITACHI SU8000)	Crystalline phase, surface composition, and elemental analysis	Japan
Zeta Potential and Submicron Particle Size Analyzers (Beckman Coulter Delsa™Nano C)	Measure particle size and zeta potential of particles	USA

3.5.2 Analysis of humic acid

The content of NOMs was based on the mineralization of dissolved organic carbon (DOC) and reduction of UV absorbance at wavelength 254 nm (UV_{254}) (unsaturated and aromatic carbon contents). UV_{254} was measured with a spectrophotometer (U-2800A, Hitachi, Japan) and DOC was determined by a wet oxidation TOC analyzer (1010W, Systematic, Taiwan).

Table 3-5. The instrument and reagent for analysis of humic acid.

UV Absorbing (UV_{254})			
Instrument	Function		Country
UV/Vis Double Beam spectrophotometer (Hitachi U-2800A)	Quantity of double bond organic matters		Japan
Dissolved organic carbon (DOC)			
Instrument	Function		Country
Total organic carbon analyzer (Wet Oxidation-TOC) (1010W, Systematic)	Quantity of dissolved organic carbon		Taiwan
Reagent	Cas/Catalog/HS number	Makers	Country
Sodium persulfate ($Na_2S_2O_8$)	7775-27-1	Merck	Germany
Phosphoric acid (H_3PO_4)	7664-38-2	Merck	Germany
Potassium hydrogen phthalate (KHP)	877-24-7	Merck	Germany
Sodium carbonate (Na_2CO_3)	497-19-8	Merck	Germany
Stock solution: 2.128 g KHP in 1 L reagent water (1,000 mg C/L)			
Calibration Equation (2011.11.16): $y = 15217x + 3449$ ($R^2 = 0.999$), MDL: 0.06 mg/L (n = 3)			

3.5.3 Analysis of hydroxyl radical scavengers

The HPLC system with reverse phase column for the chromatographic analysis is consisted of a PU-980 type pump (Jasco Co., Japan) and an UV-975 type detector and. The column is a Pharmacia C_2-C_{18} μRPC column ST 4.6/100 (5 um, 4 mm ID x 15 cm) with and volume of 1.66mL. For all HPLC analysis , the elution solution consisted of methanol and deionized water (V/V=70:30) was used with flow rate of 0.5 mL/min. The absorbance of coumarin and 7-hydroxycoumarin were measured at wavelength 320 nm, which was chosen due to obtain the maximum sensitive detection.

Table 3-6. The instrument and reagent of analysis of hydroxyl radicals scavengers.

Instrument	Specification and Operation Conditions		
High performance liquid chromatography (HPLC, Jasco Co., Japan)	Detector: UV-975 Pump: PU-980 Column: Pharmacia C_2-C_{18} μRPC column ST 4.6/100 Colum volume: 1.66 mL DI water flow rate: 0.5 mL/min Filtration: 0.45 μm membrane Injection loop: 300 μL		
Reagent	Cas/Catalog/HS number	Maker	Country
Methanol (CH_3OH)	67-56-1	Merck	Germany
Coumarin ($C_9H_6O_2$)	91-64-5	Merck	Germany
7-hydroxycoumarin ($C_9H_6O_3$)	93-35-6	Merck	Germany
tert-Butyl alcohol (TBA)	75-65-0	Merck	Germany
Calibration equation of coumarin (2012.6.15): $y= 1.29\times10^{-5}x - 6.01\times10^{-1}$, $R^2 = 0.999$, MDL = 0.04 mg/L (n= 7) Calibration equation of 7-hydroxycoumarin (2012.6.15): $y= 4.03\times10^{-6}x–1.823\times10^{-2}$, $R^2 = 0.999$, MDL = 0.01 mg/L (n=7)			

Chapter 4 Result and Discussion

4.1 Characterization of the assembled and reused catalysts

TEM and SEM images of assembled catalysts ($Fe_3O_4/SiO_2/Ag$) are presented in Figs. 4-1 to 4-4. It can be clearly seen that these nanoparticles have observed as well-shaped spherical. The average diameter of the $Fe_3O_4/SiO_2/Ag$ nanoparticle is around 20-25 nm. In addition, the catalyst after ozonation remained the same spherical structure and particle size. Elements of qualitative and semi-quantitative analysis of catalyst by EDS is shown in Tables 4-1 and 4-2. The atomic percentage of O, Si, Fe and Ag are 79.09, 11.31, 7.95 and 1.65, respectively. Even after the ozonation, the atomic percentage of the particles did not change significantly (O, Si, Fe and Ag are 74.06, 9.03, 15.29 and 1.62%). The results of TEM, SEM and EDS indicated that the assembled catalyst are with good chemical stability. The field-dependent magnetizations of various composite spheres (i.e., Fe_3O_4, Fe_3O_4/SiO_2 and $Fe_3O_4/SiO_2/Ag$) were analyzed by using SQUID. Fig. 4-5 shows that all the structure (Fe_3O_4, Fe_3O_4/SiO_2 , $Fe_3O_4/SiO_2/Ag$ and $Fe_3O_4/SiO_2/Ag$ (reuse)) presented the superparamagnetic phenomenon at room temperature (25℃) and the magnetization are about 77.2, 47.6, 31.7 and 25.4 emu/g. Comparison of previous studies (Feng *et al.*, (2010), Li *et al.*, (2010), Wang *et al.*, (2010) and Lu, (2011)), the particles synthesized ($Fe_3O_4/SiO_2/Ag$) in this study are with higher magnetization and smaller particle size than previous works (Table. 4-3), which means a better recovery and dispersion in the system.

Reduction of the saturation magnetization is due to the metal on the catalyst surface are makes the dipole interaction decreased. Fig. 4-6 indicated the catalysts with good dispersion in water and can be easily recovered using magnets.

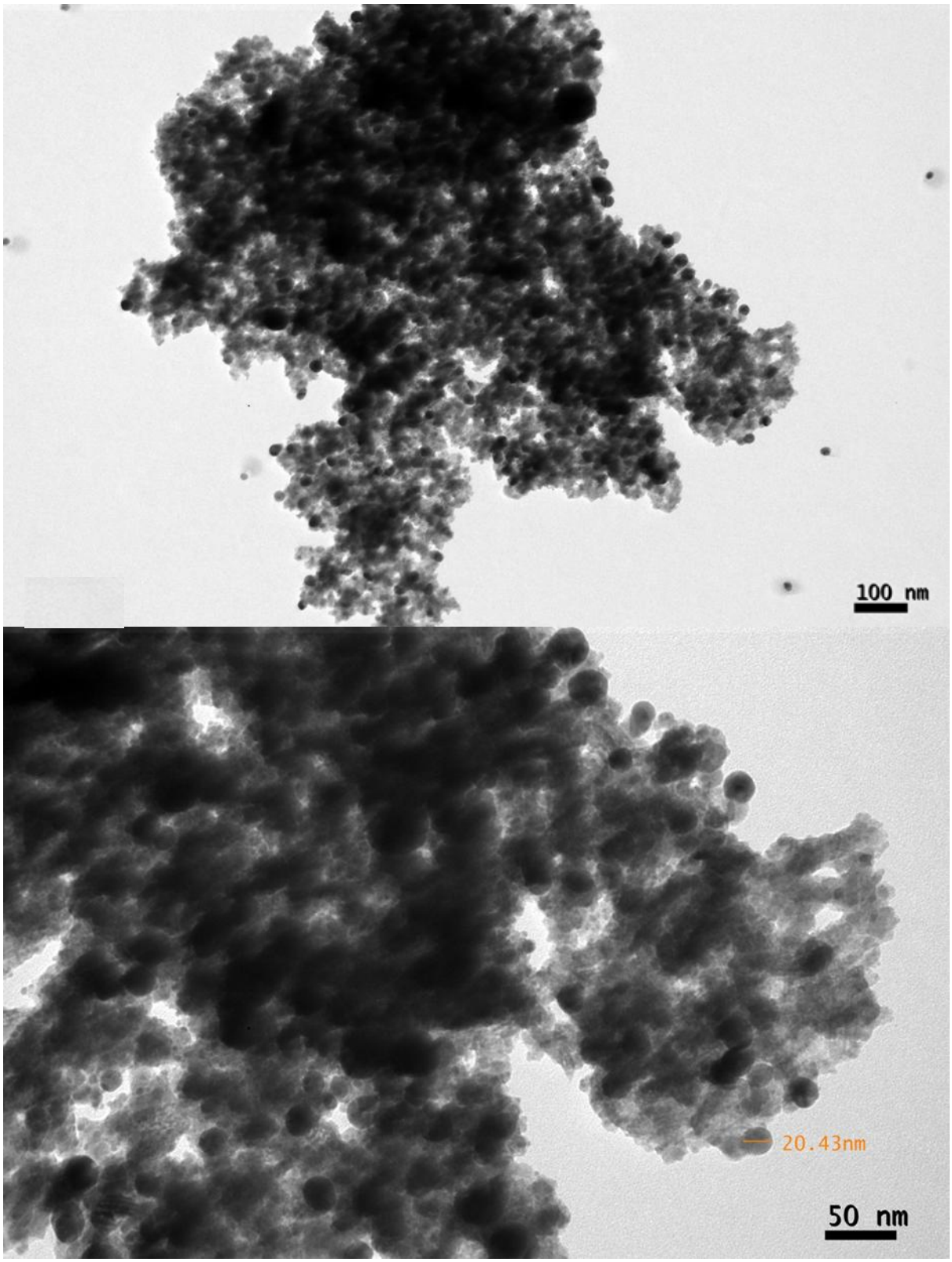

Fig. 4-1. TEM images of catalyst ($Fe_3O_4/SiO_2/Ag$).

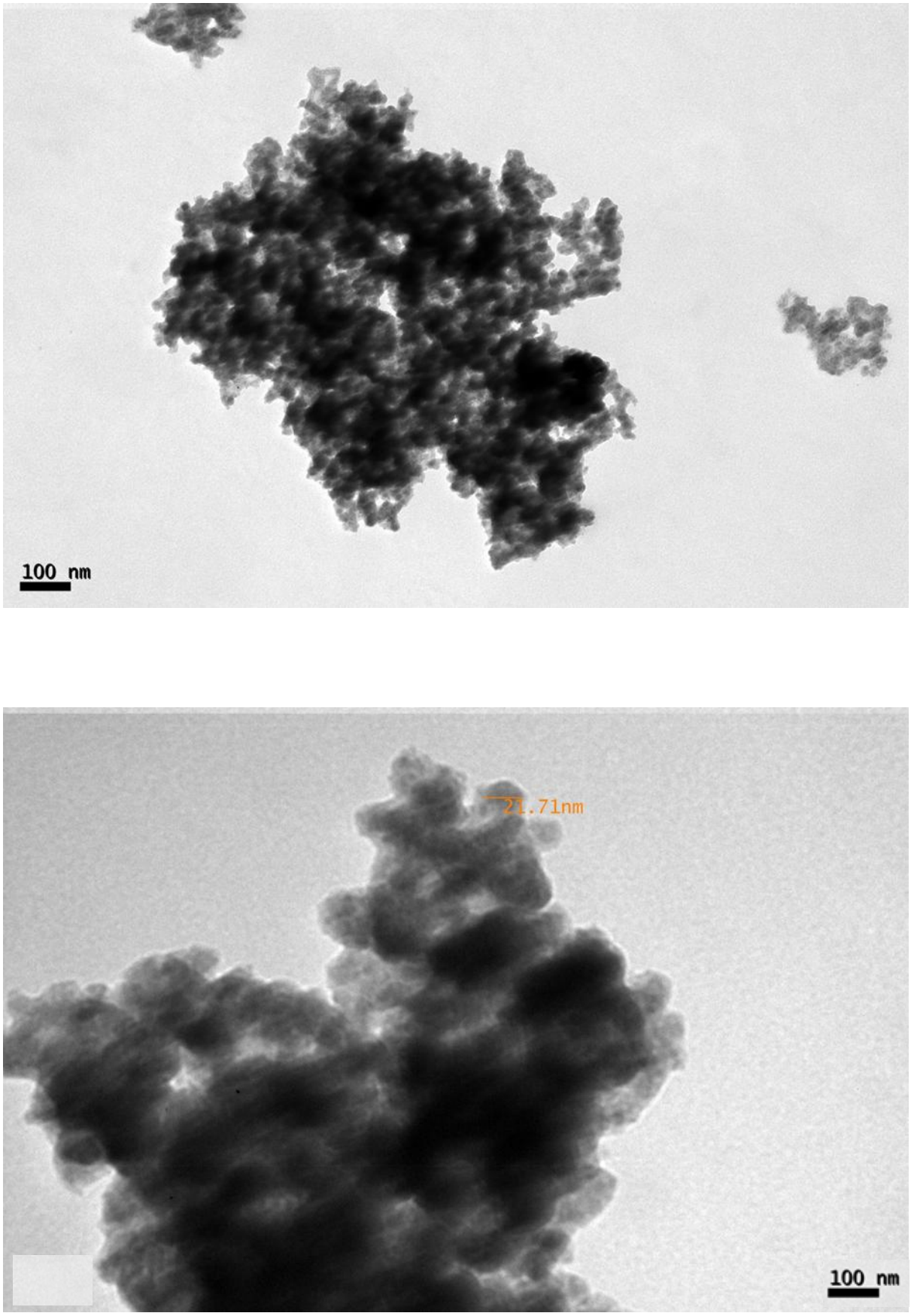

Fig. 4-2. TEM images of catalyst ($Fe_3O_4/SiO_2/Ag$) after ozonation.

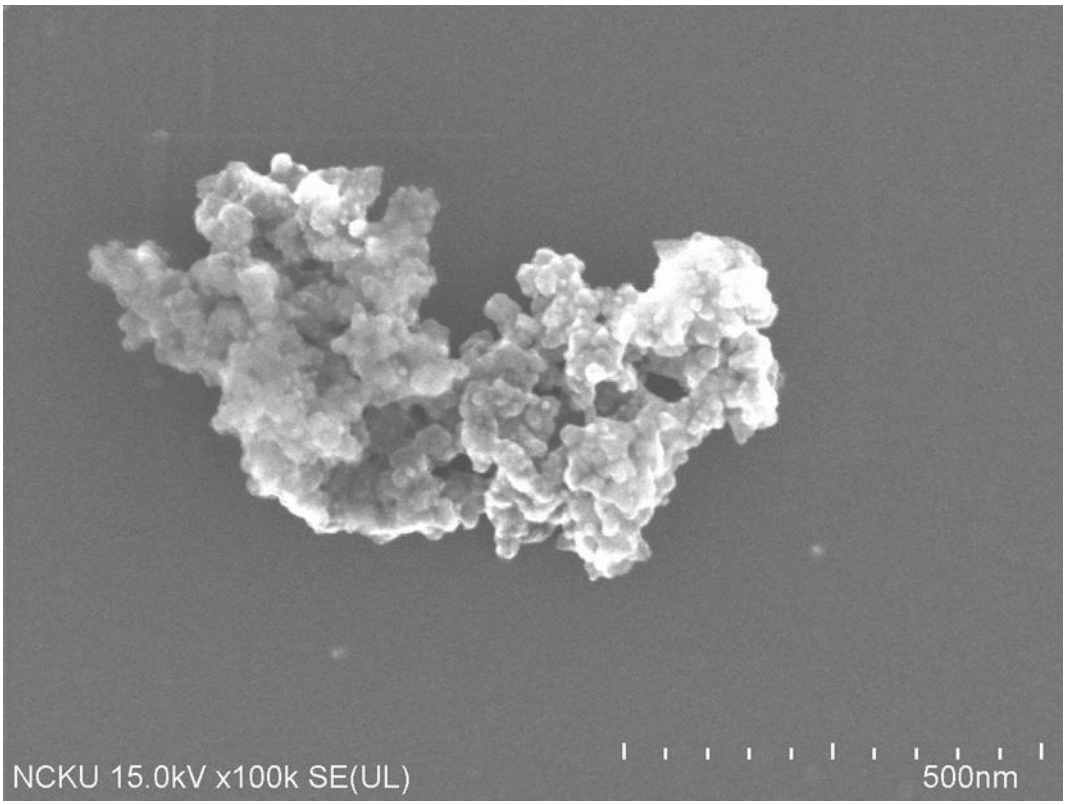

Fig. 4-3. SEM images of catalyst ($Fe_3O_4/SiO_2/Ag$).

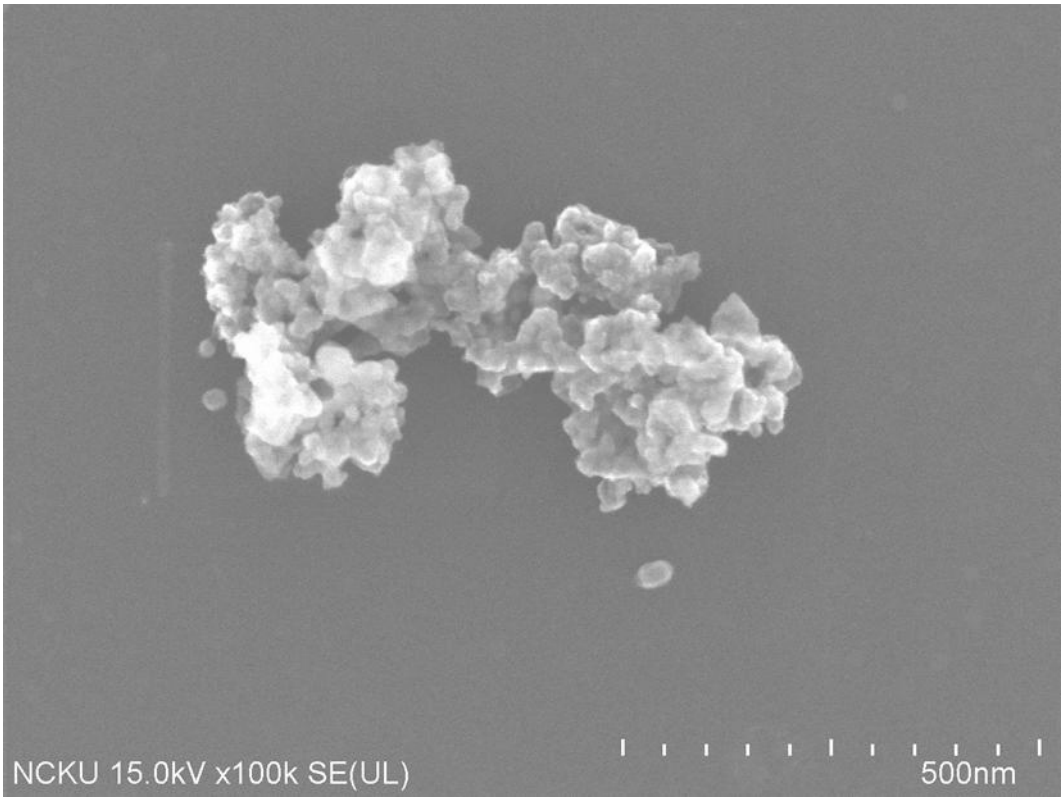

Fig. 4-4. SEM images of catalyst ($Fe_3O_4/SiO_2/Ag$) after ozonation.

Table 4-1. Elements of qualitative and semi-quantitative analysis of magnetic catalyst.

El	AN	Series	unn. C [wt. %]	norm. C [wt. %]	Atom. C [at. %]	Error [wt. %]
O	8	K-series	28.90	57.38	79.09	4.8
Si	14	K-series	7.25	14.40	11.31	0.4
Fe	26	K-series	10.14	20.14	7.95	0.5
Ag	47	L-series	4.07	8.07	1.65	0.2
		Total:	50.36	100.00	100.00	

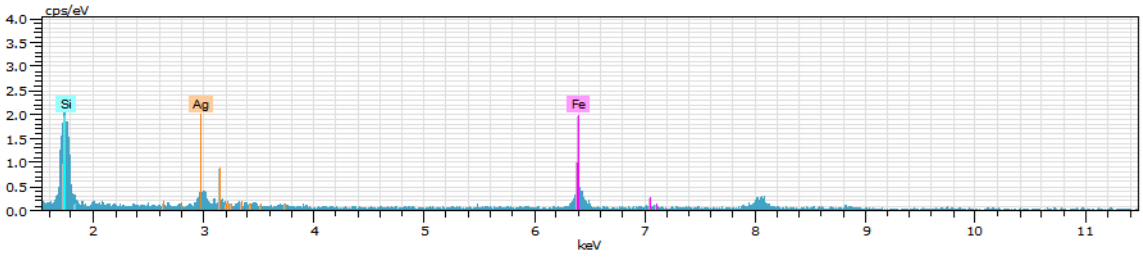

Table 4-2. Elements of qualitative and semi-quantitative analysis of magnetic catalyst after ozonation.

El	AN	Series	unn. C [wt. %]	norm. C [wt. %]	Atom. C [at. %]	Error [wt. %]
O	8	K-series	49.42	48.03	74.06	6.4
Si	14	K-series	10.57	10.28	9.03	1.2
Fe	26	K-series	35.62	34.62	15.29	0.5
Ag	47	L-series	7.27	7.07	1.62	0.3
		Total:	50.36	100.00	100.00	

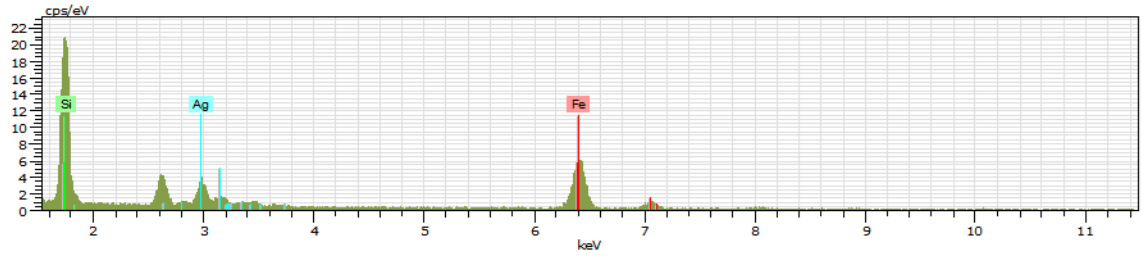

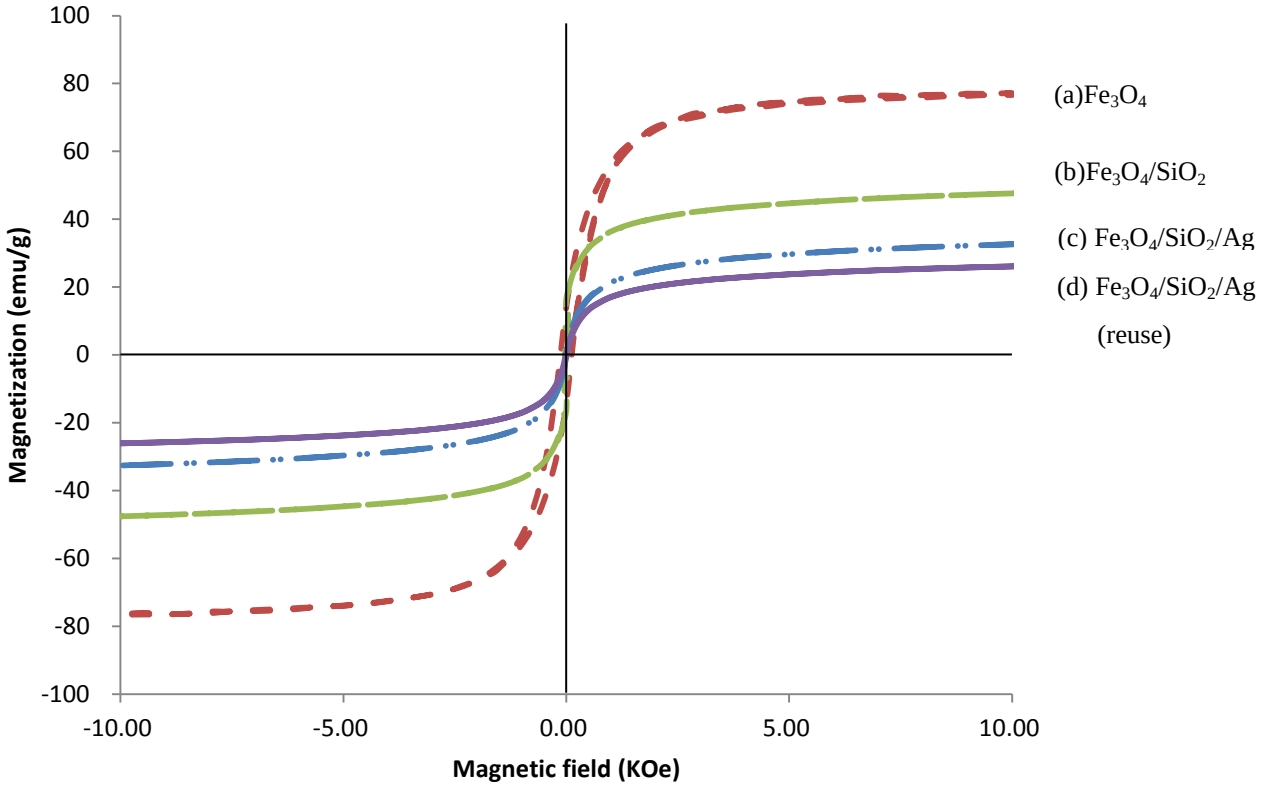

Fig. 4-5. Field-dependent magnetization hysteresis of (a)Fe_3O_4, (b)Fe_3O_4/SiO_2, (c)$Fe_3O_4/SiO_2/Ag$ and (d) $Fe_3O_4/SiO_2/Ag$ (resue) at 25℃.

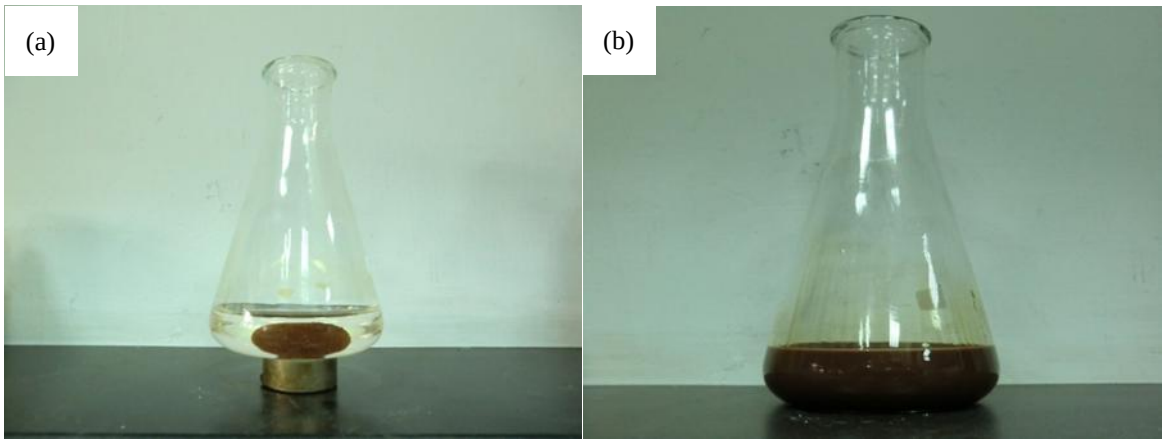

Fig. 4-6. Photographs the respective catalyst dispersed in water (a) with and (b) without external magnetic field.

Table 4-3. The comparison of magnetic particles in different references.

Reference	Particle structure	Particle size (nm)	Magnetization (emu/g)
Feng *et al.* (2010)	Fe_3O_4/SiO_2-GPTMS-Asp-Co	215	15.0
Li *et al.* (2010)	Fe_3O_4/SiO_2/Au	130	17.1
	Fe_3O_4/SiO_2/Au-Ag	470	15.0
Wang *et al.* (2011)	Fe_3O_4/SiO_2/PbS	545	26.0
Lu (2011)	Fe_3O_4/SiO_2/Co	110	6.3
This study (2012)	Fe_3O_4/SiO_2/Ag	25	31.7

4.2 The mechanisms of silver magnetic nanoparticles catalytic ozonation

In this study, in order to investigate the catalytic ozonation mechanisms of decompose NOMs, coumarin (COU) was selected as target compound to conduct the following study, while TBA will be adapted to compare the effect with coumarin. The catalyst was a modified magnetic silver magnetic nanoparticles ($Fe_3O_4/SiO_2/Ag$), which can easily be recovered under magnetic condition.

Coumarin is one of the effective free radical scavengers, which can be used to catch and measure the oxidation capability in ozonation reaction. Subtract the overall ozonation to the ozone direct reaction, it can obtain ozone indirect reaction. Normally, coumarin may react with free radical and generate 7-hydroxycoumarin as intermediate, therefore it be used as the probe molecule to measure the amount of free radicals in system. Among all, tert-Butyl alcohol (TBA) also is one of the famous $\bullet$OH scavengers and with a high reaction rate (6×10^8 $M^{-1}S^{-1}$) (Ikhlaq *et al.*, 2012). In ozonation process, the excess amount of scavenger may trap all $\bullet$OH and push the system toward ozone direct reaction.

4.2.1 Zeta potential and pH_{PZC} of catalyst

In the heterogeneous catalytic ozonation systems, pH is the most important factor which will not only affect the decomposition of ozone but also determines the reaction of the catalyst surface. When pH of the solution is higher than pH_{PZC} of catalyst, the surface of catalyst is negatively charged (no surface hydroxyl groups present). While pH of the solution is lower than pH_{PZC} of catalyst, the surface of catalyst is positively charged, and pH of the solution is equal to pH_{PZC} of catalyst, then the surface of catalyst is neutral.

As shown in Fig. 4-7, the zeta potential of silver magnetic nanoparticles ($Fe_3O_4/SiO_2/Ag$) decreases from 27.67 to -57.92 mV with the pH value increasing from 3 to 11, indicating that the surface charge of silver magnetic nanoparticles changes from positive to negative. The pH_{PZC} of silver magnetic nanoparticles is found to be 3.8. The catalysts used for heterogeneous catalytic ozonation were listed in Table 4-4. The pH_{PZC} were obtained between 1.8 to 9.8, while in this case a pH_{PZC} 3.8 was found in this study. Previous studies have confirmed that the catalytic ozonation is only suitable in the aqueous solution at acidic conditions. However, the reaction of ozone with organic matter on the catalyst surface will also affect the degree of organic matter removal. Therefore, the smaller pH_{PZC} value of catalyst, not only the more conducive to catalysts react with ozone, but also suitable for the catalytic ozonation. Due to the pH_{PZC} value of $Fe_3O_4/SiO_2/Ag$ is 3.8, the results show that the $Fe_3O_4/SiO_2/Ag$ is more suitable than the other catalysts (Table 4-4) in catalytic ozonation.

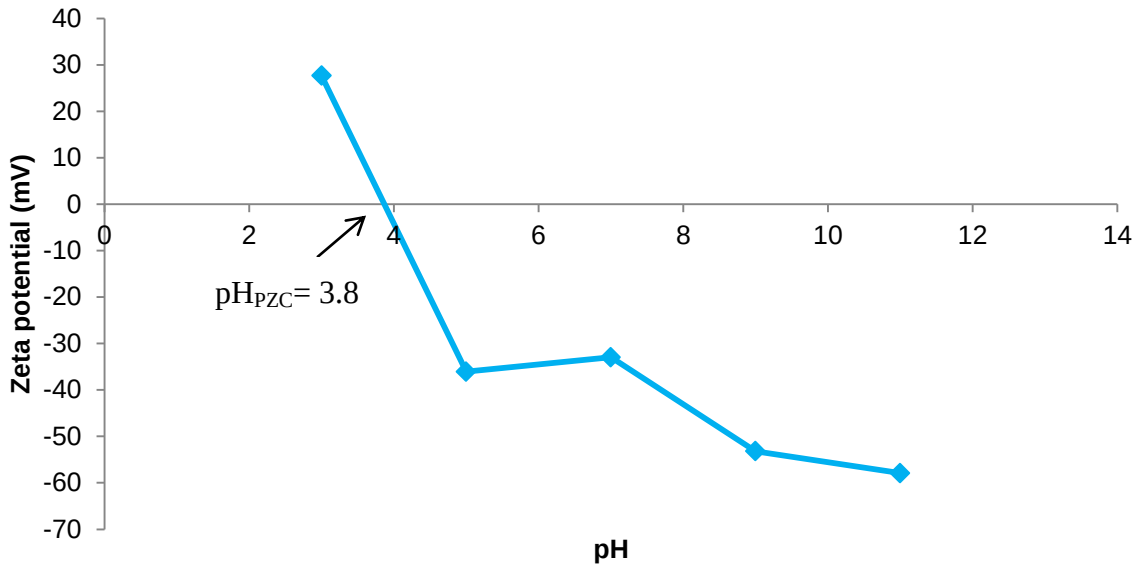

Fig. 4-7. The zeta potential values of $Fe_3O_4/SiO_2/Ag$ (pH 3, 5, 7, 9 and 11) and with pH_{PZC} of 3.8.

Table 4-4. The pH_{PZC} of catalysts used for Heterogeneous catalytic ozonation.

Reference	Target pollutant	catalyst	pH_{PZC}
Li *et al.* (2011)	Pyruvic acid	CeO_2	6.3
		PdO/CeO_2	5.4
Pocostales *et al.* (2011)	Pharmaceuticals (Sigma–Aldrich Inc.)	γ-Al_2O_3 (Alcoa Inc., USA).	8.1
		Co_3O_4/Al_2O_3	7.9
Lu (2011)	Humic acid (Aldrich Chemistry)	$Fe_3O_4/SiO_2/Co$	1.8
Sui *et al.* (2012)	Ciprofloxacin (NICPBP, China)	MWCNTs (Shanghai ANT, Co., Ltd.)	4.7
		MnOx/MWCNT	4.2
		MnOx	3.9
Guzman-Perez *et al.* (2012)	Atrazine (Sigma–Aldrich Inc.)	AC (Norit, Alfa Aesar)	9.8
		AC (F-400, Calgon Carbon Corp.)	9.3
This study (2012)	Humic acid (Aldrich Chemistry)	$Fe_3O_4/SiO_2/Ag$	3.8

4.2.2 Catalytic ozonation of coumarin

Catalytic ozonation of coumarin has been used to differentiate between radical and non radical reaction. Due to the reaction of coumarin with • OH will produce specific intermediate (7-hydroxycoumarin) (Ikhlaq *et al.*, 2012), therefore the amount of 7-hydroxycoumarin generation can be used to indicate the content of the • OH. Catalytic ozonation experiments were conducted at T= 25℃ in a semi-batch reactor. The pH of coumarin solution was adjusted to 3, 5, 7, and 9. Coumarin solution (100 mg/L) was transferred to the reactor containing 50 mg/L of the catalyst ($Fe_3O_4/SiO_2/Ag$) and was stirred (at 500 rpm) over a period of 30 min.

4.2.3 Effect of pH

The pH of the solution will affect the reaction of ozone in water. At low pH cases, the removal rate of both ozone alone and ozone with $Fe_3O_4/SiO_2/Ag$ have higher value than those at high pH cases (Fig. 4-8). While the coumarin removal rate have highest value of 98% of ozone alone and 78% of ozone with $Fe_3O_4/SiO_2/Ag$ at pH 3 (Fig. 4-8 a). This is due to massive ozone self-decomposition at high pH cases (Nawrocki and Kasprzyk-Hordern, 2010), caused the coumarin removal rate lower than low pH cases.

4.2.4 Effect of catalyst doses

The presence of $Fe_3O_4/SiO_2/Ag$ caused the coumarin removal rate reduction at all pHs cases (Figs. 4-8a to 4-8d). This is due to ozone is decomposed by $Fe_3O_4/SiO_2/Ag$ leading to • OH generation. The more coumarin removal implies the more ozone in the reactor, while the more 7-hydroxycoumarin generation indicates the more • OH exists. Comparing the generation of 7-hydroxycoumarin under pH 3, 5 and 7, the $Fe_3O_4/SiO_2/Ag$ improve the production of 7-hydroxycoumarin than those without $Fe_3O_4/SiO_2/Ag$ cases (Fig. 4-8a′, 4-8b′ and 4-8c′). This results shows that the $Fe_3O_4/SiO_2/Ag$ can increase the • OH generation. While due to the strong ozone self-decomposition at pH 9, leading to $Fe_3O_4/SiO_2/Ag$ and coumarin complitively grab • OH. Therefore, the effect of the catalyst is inhibited, making the generation of 7-hydroxycoumarin reduced (Fig. 4-8d′).

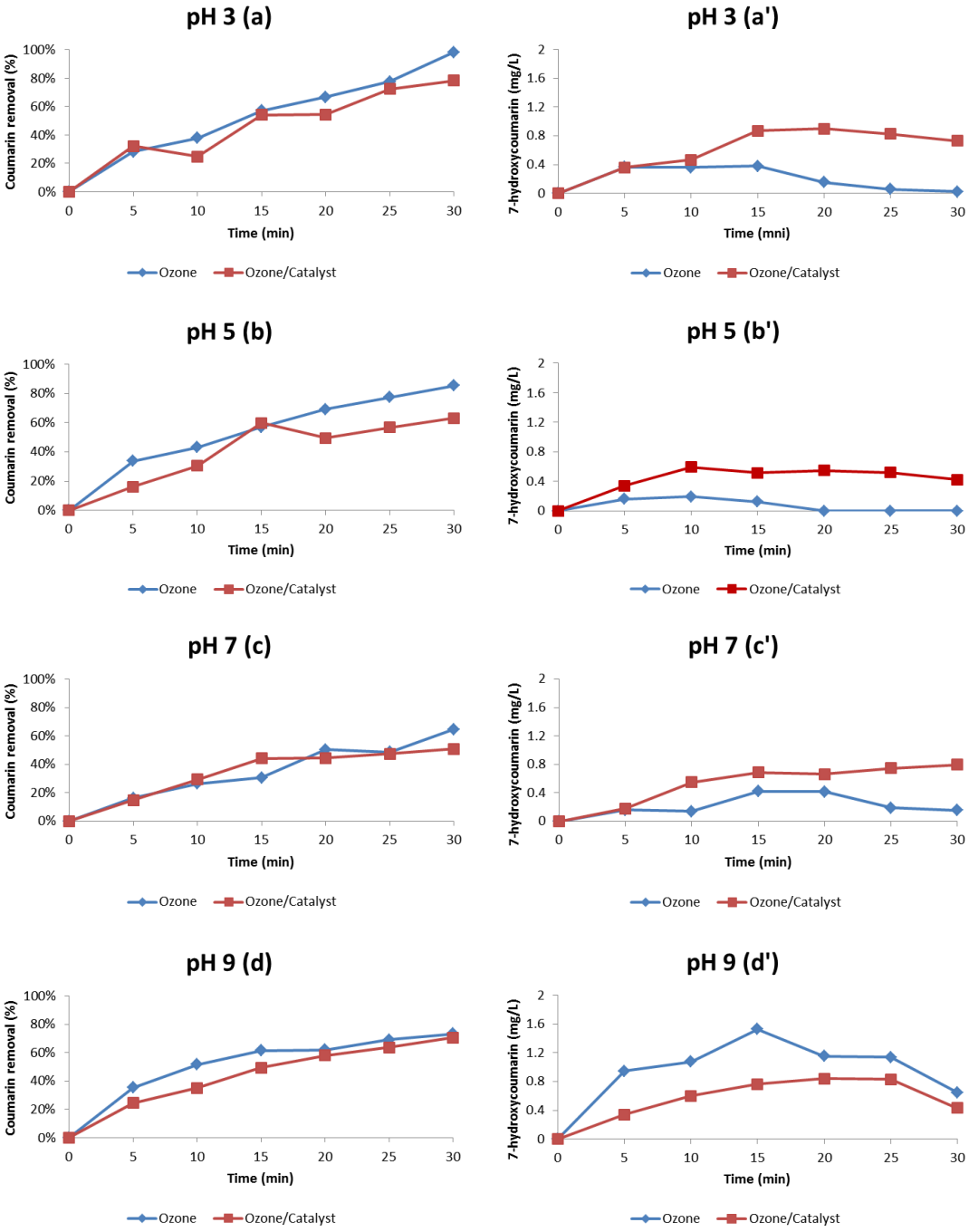

Fig. 4-8. The coumarin removal (a) pH 3, (b) pH 5, (c) pH 7 and (d) pH 9 and 7-hydroxycoumarin generation (a′) pH 3, (b′) pH 5, (c′) pH 7 and (d′) pH 9 in the catalytic ozonation under various pHs with and without catalyst (O_3 concentration of 0.6 mg/L, COU and TBA both of 100 mg/L, catalyst doses of 50 mg/L of $Fe_3O_4/SiO_2/Ag$ and T=25℃).

4.2.5 Effect of TBA

By comparing the difference of 7-hydroxycoumarin generation between ozone alone and ozone with catalyst, $Fe_3O_4/SiO_2/Ag$ is most effective at pH 5 (Fig 4-8). In order to further verify the presence of • OH, 100 mg/L of TBA was added into catalytic ozonation system at pH 5. In other words, the presence of TBA will give priority to consumption of • OH, leading to reduced the reaction of coumarin with • OH in the catalytic ozonation system. Fig. 4-9 indicates the 7-hydroxylcoumarin profiles under different operation cases: ozone, ozone/catalyst, ozone/TBA, ozone/catalyst/TBA, under initial pH of 5, O_3 concentration of 0.6 mg/L, coumarin of 100 mg/L, catalyst dose of 50 mg/L and T=25℃. The $Fe_3O_4/SiO_2/Ag$ may enhance the decomposition of ozone and come out more • OH than the system without it. While the dose of scavenger may catch free radical and reduce the output of 7-hydroxycoumarin. Among all, the system ozone/TBA came nothing 7-hydroxycoumarin out due to non • OH was found in the reactor, i.e., excess TBA caught all • OH. In the ozone only system, it came out some 7-hydroxycoumarin found in Fig. 4-9. It implies there are some • OH in the system and generate the intermediate. While system ozone/TBA , the excess TBA consumed all • OH s in the system, i.e., no indirect reaction occurred, therefore no 7-hydroxycoumarin was found in it.

The sole ozone and ozone/catalyst systems indicating a significantly difference of 7-hydroxycoumarin intermediate due to the 50 mg/L Ag catalyst reaction. The similar difference between ozone/catalyst/TBA

and ozone /TBA also found in Fig. 4-9. Theoretically, the Ag catalyst may decompose ozone to generate • OH, i.e., the more • OH s in reactor, the more 7-hydroxycoumarin came out. The intermediate 7-hydroxycoumarin indicates the indirect reaction capability taking place in the ozone with catalyst system and with the trend of ozone /catalyst > ozone/catalyst/TBA> ozone> ozone /TBA.

The online ozone monitor profiles for coumarin/ozone, coumarin/ozone/catalyst, coumarin/ozone/TBA and coumarin/ozone/catalyst/TBA were shown on Fig. 4-10. Since TBA is another scavenger, which can catch • OH in the reaction and brought the aqueous ozone level to as low as 0.2 mg/L in the system.

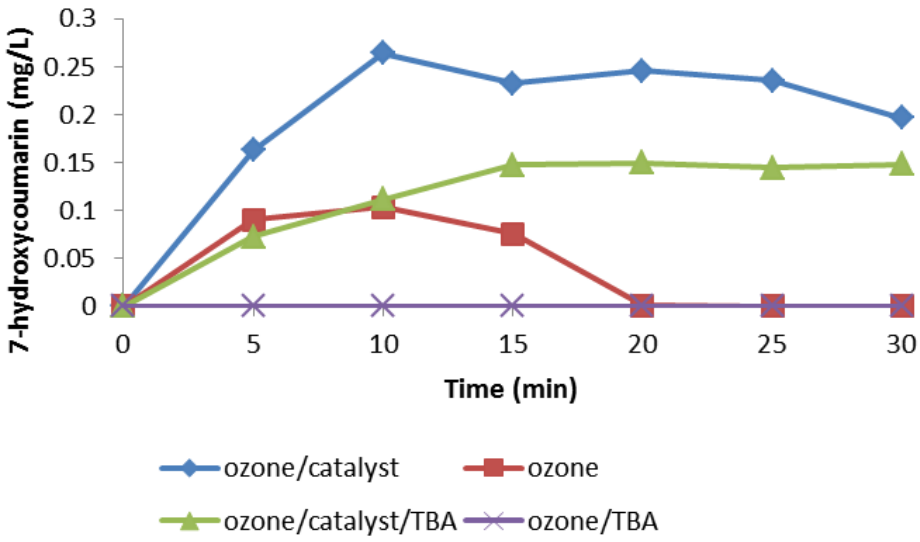

Fig. 4-9. Formation of 7-hydroxycoumarin as a result of COU and TBA in the catalytic ozonation (initial pH of 5, O_3 concentration of 0.6 mg/L, COU and TBA both of 100 mg/L, catalyst doses of 50 mg/L and T=25℃).

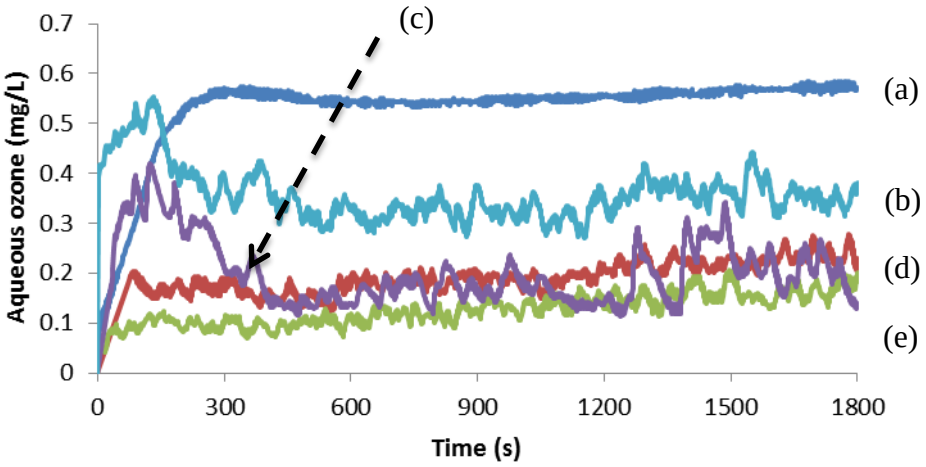

Fig. 4-10. Online aqueous ozone concentration during catalytic ozonation system, (a) deionized water, (b) ozone/coumarin, (c) ozone/coumarin/catalyst, (d) ozone/coumarin/TBA and (e) ozone/coumarin/catalyst/TBA (initial pH of 5, O_3 concentration of 0.6 mg/L, COU and TBA both of 100 mg/L, catalyst doses of 50 mg/L and T=25℃)

4.2.5 Reuse of the catalyst

In order to investigate the $Fe_3O_4/SiO_2/Ag$ reusability, the ozone decomposition experiments were conducted in deionized water at *T*= 25℃, catalyst dose of 50 mg/L and recovery $Fe_3O_4/SiO_2/Ag$ with magnet (because the particles are magnetic materials). The results (Fig. 4-11) showed that $Fe_3O_4/SiO_2/Ag$ recovery after five times still retains the ability of ozone decomposition.

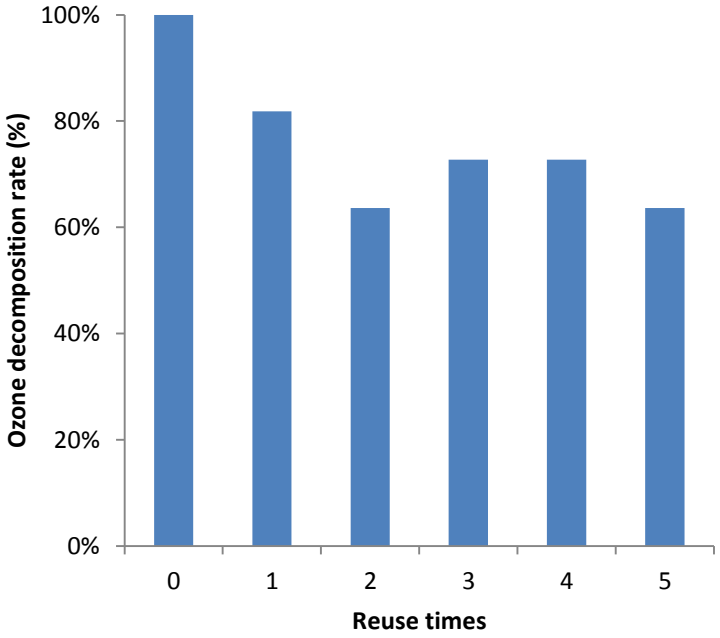

Fig. 4-11. Reusability of $Fe_3O_4/SiO_2/Ag$ to decompose ozone (*T*=25℃, initial pH of 5, O_3 concentration of 0.6 mg/L, catalyst doses of 50 mg/L, $Fe_3O_4/SiO_2/Ag$ for reuse 5 times).

4.3 Catalytic ozonation of humic acid

To degradation of natural organic matters (NOMs) with catalytic ozonation, humic acid (HA) was used in this study. The typical molecule structure of humic acid is a mixture of aromatic nuclei with phenolic and carboxylic substituents (Chang, 2010). HA can be analyzed by spectrophotometer (U-2800A, Hitachi Co., Japan) at wavelength of 254 nm. While dissolved organic carbon (DOC) concentration can be used to indicate the degree of mineralization of organic matters (Roccaro and Vagliasindi, 2009).

4.3.1 Degradation of humic acid and effect of pH

Ozonation experiments were conducted at 25℃ in a semi-batch reactor. The pH of HA solution was adjusted to 4, 7 and 10 (acidic, neutral and alkaline conditions). Initial HA solution of 20 mg/L was stirred (at 500 rpm) over a period of 30 min. The removal rate constants (Table 4-5) indicated that with the increase pH of the solution will promote the ozone conduct indirect reaction (radical-type reaction), which means the removal rate constant of HA will be increased. Compare to ozone, the removal rate constant increase in the pH 4, while in pH 7 and 10 both are decreasing. This is due to the self-decomposition of ozone with the pH 7 and 10 (Fig. 4-12). In this case, ozone decomposed to • OH, which occupied the surface of catalyst and interfere the oxidation. Hence a reduction of HA removal was found in high pH case (Li *et al.*, 2011). It is also indicated that in contrast to ozonation alone system, the catalytic ozonation allows the effective formation of • OH at a low pH (Nawrocki and

Kasprzyk-Hordern, 2010).

Table 4-5. The first-order HA removal rate constant in catalytic ozonation under various pH cases: 4, 7 and 10.

Ozonation system	pH	K_d (s^{-1})	R^2
Ozone	4	6.0×10^{-4}	0.881
Ozone/catalyst*	4	8.0×10^{-4}	0.992
Ozone	7	1.0×10^{-3}	0.958
Ozone/catalyst*	7	8.0×10^{-4}	0.866
Ozone	10	1.2×10^{-3}	0.980
Ozone/catalyst*	10	7.0×10^{-4}	0.863

Catalyst*: $Fe_3O_4/SiO_2/Ag$ (50 mg/L)

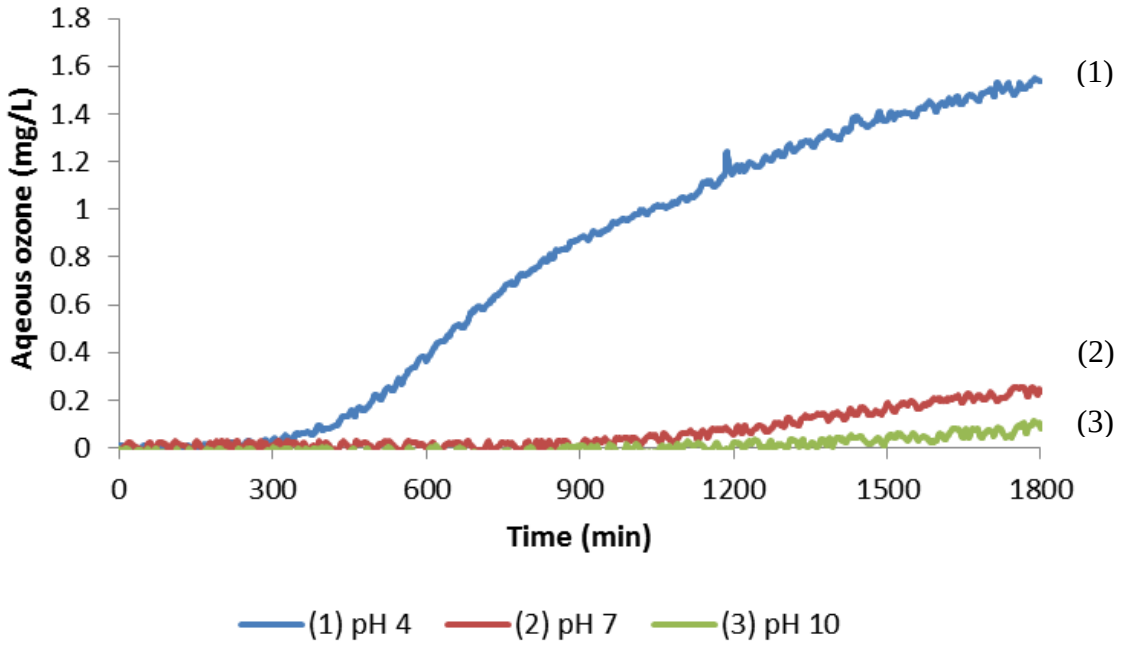

Fig. 4-12. Online aqueous ozone concentration profiles during ozonation under various pH cases: (1) 4 , (2) 7 and (3) 10 (HA of 20 mg/L, O_3 concentration of 1.6mg/L and T= 25℃).

4.3.2 Effect of catalyst doses

Catalytic ozonation experiments were conducted at 25℃ in a semi-batch reactor. The initial HA solution of 20 mg/L was transferred to the reactor containing 0, 5, 25 and 50 mg/L of the catalyst and was stirred at 500 rpm over a period of 60 min. Fig. 4-13 indicated the highest HA removal rate constant is at the 50 mg/L of catalyst dose case. Normally, the catalyst in the system used to decompose of ozone for generate free radical and enhance the oxidation capability. While in high dose (100 mg/L) of catalyst, since there are not sufficient ozone in the system, therefore less free radical came out than normal case, therefore it cannot obtain high removal rate constant (K_d).

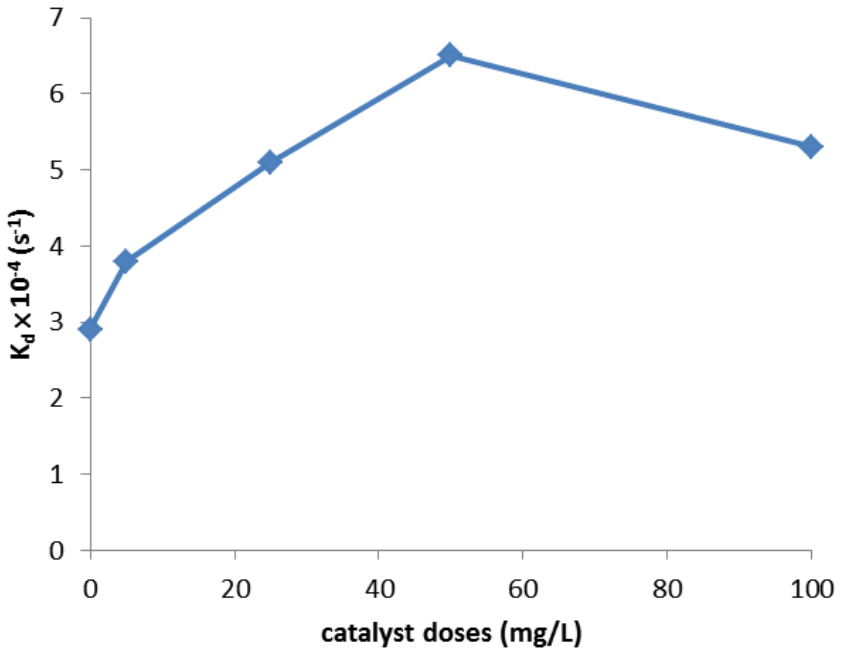

Fig 4-13. HA removal rate constants of catalytic ozonation (initial pH of 4, O_3 concentration of 1.6mg/L, initial HA of 20 mg/L, catalyst doses of 5, 25, 50 and 100 mg/L and *T*= 25℃).

4.3.3 Mineralization rate of humic acid

The mineralization rate of HA could be analyzed by TOC analyzer. Catalytic ozonation experiments were conducted at *T*= 25℃ in a semi-batch reactor. Initial HA concentration of 20 mg/L was transferred to the reactor containing 0, 5, 25 and 50 mg/L of the catalysts and stirred at 500 rpm over a period of 30 min. The results (Fig. 4-14) showed the mineralization rate of catalytic ozonation was more effective than ozonation alone, while the similar results were also observed in a previous study (Chen *et al.*, 2011 and Sui *et al.*, 2012). This is because ozonation alone on organic matter mineralization capacity is limited, while the catalytic ozonation can mineralize the organic matters based upon the DOC profiles.

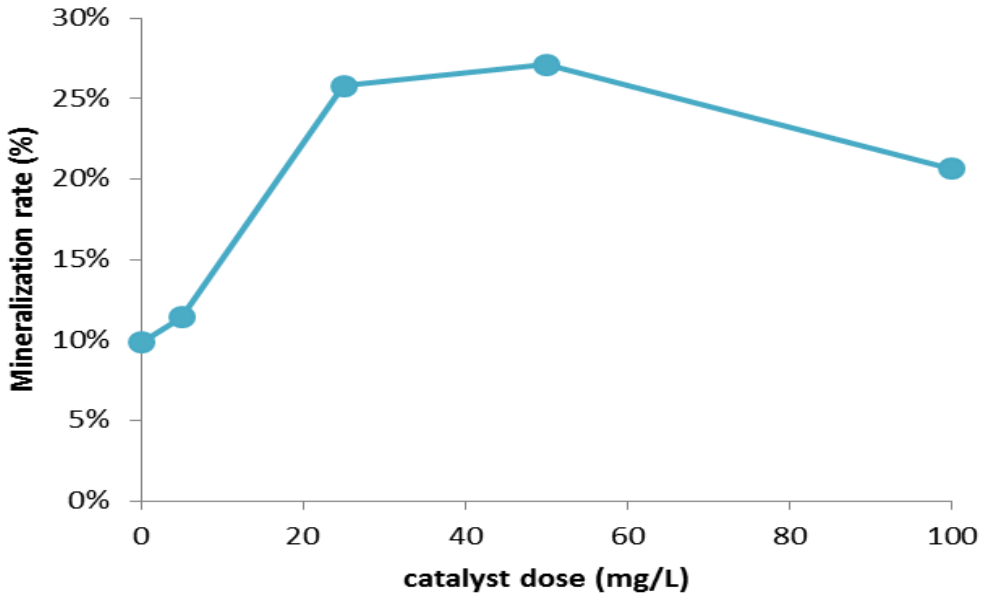

Fig. 4-14. Mineralization rate of HA based on DOC by ozonation and catalytic ozonation (initial pH of 4, O_3 concentration of 1.6mg/L, initial HA of 20 mg/L, catalyst doses of 0, 5, 25, 50 and 100 mg/L and *T*= 25℃

4.3.4 Kinetics of the decay of aqueous ozone

Aqueous ozone decay was investigated in deionized water in the semi batch reactor. Experiments was conducted at pH 4 (in order to inhibit the strong self-decomposition of ozone). A solution of ozone was prepared in water by introducing ozone (until a saturation concentration of ozone of 1.6 mg/L) in semi-batch reactor. A 0.05g/L of $Fe_3O_4/SiO_2/Ag$ catalyst was stirred at 500 rpm over a period of 30 min.

Table 4-6 indicated the first-order ozone decay rate constants in several ozonation systems. Based upon the first-order kinetics, the K_d values were 4×10^{-4} s^{-1} for ozone alone and 7×10^{-4} s^{-1} for catalytic ozonation in this study, it also indicates the K_d value of $Fe_3O_4/SiO_2/Ag$ is 1.75 times than that of ozone alone system. The dose of $Fe_3O_4/SiO_2/Ag$ of 0.05 g/L is much lower than other catalysts (Table 4-6), however, the K_d value is only less than the FeOOH of 9.3×10^{-4} s^{-1}. The results showed that $Fe_3O_4/SiO_2/Ag$ is an economical and efficient catalyst.

Table 4-6. The comparison of the first-order ozone decay rate constants in different ozonation system with deionized water.

Reference	pH	Ozonation system	O_3 con. (mg/L)	Catalyst dose (g/L)	K_d (s^{-1})
Park	4	O_3	2	-	4.2×10^{-4}
et al.,	4	O_3/FeOOH	2	2	9.3×10^{-4}
(2004)					
Lu (2011)	4	O_3	1.6	-	4.0×10^{-4}
	4	O_3/ (Fe_3O_4/SiO_2/Co)	1.6	1	5.0×10^{-4}
Ikhlaq	3	O_3	1.5-3	-	3.8×10^{-4}
et al.,	3	O_3/Alumina	1.5-3	5	6.1×10^{-4}
(2012)	3	O_3/Z25H	1.5-3	5	5.2×10^{-4}
	3	O_3/Z1000H	1.5-3	5	4.6×10^{-4}
	3	O_3/Z25Na	1.5-3	5	4.7×10^{-4}
	3	O_3/Z900Na	1.5-3	5	4.5×10^{-4}
This study	4	O_3	1.6	-	4.0×10^{-4}
(2012)	4	O_3/ (Fe_3O_4/SiO_2/Ag)	1.6	0.05	7.0×10^{-4}

Chapter 5 Conclusions and Suggestions

5.1 Conclusions

1. The catalyst ($Fe_3O_4/SiO_2/Ag$) synthesized in this study presented the superparamagnetic phenomenon (easy to disperse and recovery). The average diameter of the $Fe_3O_4/SiO_2/Ag$ nanoparticle is around 20-25 nm and high magnetization of 31.7 emu/g.

2. $Fe_3O_4/SiO_2/Ag$ nanoparticle is an effective catalyst for the decomposition of ozone in catalytic ozonation. The generation of intermediate (7-hydroxycoumarin) were indicated the effects of hydroxyl radicals on catalytic ozonation. While the presence of TBA (hydroxyl radical scavengers) can effectively use to differentiate between radical and non radical mechanisms.

3. The HA removal rate constant of 6.5×10^{-4} (s^{-1}) of catalytic ozonation, which great than is 2.9×10^{-4} (s^{-1}) of ozonation at pH4 (reaction time of 60 min). The mineralization rate of 27.1% of catalytic ozonation was more effective than 9.8 % of ozonation alone.

5.2 Suggestions

1. Composite magnetic metal catalysts can be effective decomposition of ozone, while the combination of support and metal will determine the catalytic efficiency. Therefore, in order to enhance the effect of catalytic ozonation, it can attempt to coated variety of metals on the support surface.

References

Badis, A., Ferradji, F.Z., Boucherit, A., Fodil, D., Boutoumi, H., (2010), "Removal of natural humic acids by decolorizing actinomycetes isolated from different soils (Algeria) for application in water purification", Desalination, Vol. 259, pp. 216-222.

Beltrán, F.J., Rivas, J., Á lvarez, P., Montero-de-Espinosa, R., (2002), "Kinetics of heterogeneous catalytic ozone decomposition in water on an activated carbon", Ozone Science & Engineering, Vol. 24, pp. 227-237.

Parilti, Neval Baycan, Uyguner, Demirel, Ceyda, S., Bekbolet, Miray, (2011), "Response surface methodological approach for the assessment of the photocatalytic degradation of NOM", Journal of Photochemistry and Photobiology A: Chemistry, Vol. 225, pp. 26-35.

Chandrasekara Pillai, K., Kwon, Tae Ouk, Moon, II Shik, (2009), "Degradation of wastewater from terephthalic acid manufacturing process by ozonation catalyzed with Fe^{2+}, H_2O_2 and UV light: Direct versus indirect ozonation reactions", Applied Catalysis B: Environmental, Vol. 91, pp. 319-328.

Chen, Yi-Hung, Hsieh, Da-Cheng, Shang, Neng-Chou, (2011), "Efficient mineralization of dimethyl phthalate by catalytic ozonation using TiO_2/Al_2O_3 catalyst", Journal of Hazardous Materials, Vol.192, pp.1017-1025.

Choi, Hyemin, Veriansyah, Bambang, Kim, Jaehoon, Kim, Jae-Duck, Kang, Jeong Won, (2010), "Continuous synthesis of metal nanoparticles

in supercritical methanol", J. of Supercritical Fluids, Vol. 52, pp. 285-291.

Chowdhury, S. and Champagne, P., (2008), "An Investigation On Parameters For Modeling Thms Formation**",** Global NEST Journal, Vol. 10, pp. 80-91.

Chowdhury, Shakhawat, Rodriguez, Manuel J., Serodes, Jean, (2010), "Model development for predicting changes in DBP exposure concentrations during indoor handling of tap water", Science of the Total Environment, Vol. 408, pp. 4733-4743.

Feng, Guodong, Hu, Daodao, Yang, Lei, Cui, Yali, Cui, Xin-ai, Li, Hong, (2010), "Immobilized-metal affinity chromatography adsorbent with paramagnetism and its application in purification of histidine-tagged proteins", Separation and Purification Technology, Vol. 74, pp. 253-260.

Figuerola, Albert, Di Corato, Riccardo, Manna, Liberato, Pellegrino, Teresa, (2010), "From iron oxide nanoparticles towards advanced iron-based inorganic materials designed for biomedical applications", Pharmacological Research, Vol. 62, pp. 126-143.

Ghosh, Sudipa, Badruddoza, A.Z.M., Uddin, M.S., Hidajat, K., (2011), "Adsorption of chiral aromatic amino acids onto carboxymethyl-β-cyclodextrin bonded Fe_3O_4/SiO_2 core–shell nanoparticles", Journal of Colloid and Interface Science, Vol. 354, pp. 483-492.

Goncalvesa, Alexandra, Silvestre-Alberob, Joaquin, Ramos-Fernandez, Enrique V., Serrano-Ruiz, Juan Carlos., Orfao, Jose J.M., Sepulveda-Escribano, Antonio, Pereira Manuel, Fernando R., (2012),

“Highly dispersed ceria on activated carbon for the catalyzed ozonation of organic pollutants”, Applied Catalysis B: Environmental, Vol. 113-114, pp. 308-317.

Guzman-Perez, Carlos A., Soltan, Jafar, Robertson, Jared, (2011), “Kinetics of catalytic ozonation of atrazine in the presence of activated carbon”, Separation and Purification Technology, Vol. 79, pp. 8-14.

Hebert, Armelle, Forestier, Delphine, Lenes, Dorothe´e, Benanou, David, Jacob, Severine, Arfi, Catherine, Lambolez, Lucie, Levi, Yves, (2010), “Innovative method for prioritizing emerging disinfection by-products (DBPs) in drinking water on the basis of their potential impact on public health”, Water Research, Vol. 44, pp. 3147-3165.

Hoigné, J. and Bader, H. (1983). Rate constants of reactions of ozone with organic and inorganic compounds in water – II. Dissociating organic compounds. Water Research, Vol. 17, pp. 185–194.

Ikhlaq, Amir, Brown, David R., Kasprzyk-Hordern, Barbara, (2012), “Mechanisms of catalytic ozonation on alumina and zeolites in water: Formation of hydroxyl radicals”, Applied Catalysis B: Environmental, Vol. 123–124, pp. 94-106.

Kasprzyk-Hordern, Barbara, Ziółek, Maria, Nawrocki, Jacek, (2003), “Catalytic ozonation and methods of enhancing molecular ozone reactions in water treatment”, Applied Catalysis B: Environmental, Vol. 46, pp. 639-669.

Kim, Kyoung-Hun and Ihm, Son-Ki, (2011), “Heterogeneous catalytic wet air oxidation of refractory organic pollutants in industrial

wastewaters: A review”, Journal of Hazardous Materials, Vol. 186, pp. 16-34.

Lamsal, Rupa, Walsh, Margaret E., Gagnon, Graham A., (2011), “Comparison of advanced oxidation processes for the removal of natural organic matter”, Water Research, Vol. 45, pp. 3263-3269.

Legube, B. and Karpel Vel Leitner, N., (1999), “Catalytic ozonation: a promising advanced oxidation technology for water treatment”, Catalysis Today, Vol.53, pp. 61-72.

Li, Ling, Choo, Eugene S.G., Tang, Xiaosheng, Ding, Jun, Xue, Junmin, (2010), “Ag/Au-decorated Fe_3O_4/SiO_2 composite nanospheres for catalytic applications”, Acta Materialia, Vol. 58, pp. 3825-3831.

Li, Weiwei, Qiang, Zhimin, Zhang, Tao, Bao, Xiaolei, Zhao, Xu, (2011), “Efficientdegradation of pyruvicacid in water by catalyticozonation with PdO/CeO_2”, Journal of Molecular Catalysis A: Chemical, Vol. 348, pp. 70-76.

Li, Ying-Sing, Church, JeffreyS., Woodhead, Andrea L., (2012), “Infrared and Raman spectroscopic studies on iron oxide magnetic nano-particles and their surface modifications”, Journal of Magnetism and Magnetic Materials, Vol. 324, pp. 1543-1550.

Lin, Hui-Chuan and Wang, Gen-Shuh, (2011), “Effects of UV/H_2O_2 on NOM fractionation and corresponding DBPs formation”, Desalination, Vol. 270, pp. 221-226.

Liu, Wenbo, Zhao, Yanmei, Chow, WK, Christopher, Wang, Dongsheng,

(2011), “Formation of disinfection byproducts in typical Chinese drinking water”, Journal of Environmental Sciences, Vol. 23, pp. 897-903.

Liu, Zheng-Qian, Ma, Jun, Cui, Yu-Hong, Zhao, Lei, Zhanga, Bei-Ping, (2011), “Factors affecting the catalytic activity of multi-walled carbon nanotube for ozonation of oxalic acid”, Separation and Purification Technology, Vol. 78, pp. 147-153.

Lv, Baoliang, Xu, Yao, Tian, Hong, Wu, Dong, Sun, Yuhan, (2010), “Synthesis ofFe_3O_4\SiO_2\Ag nanoparticles and its application in surface-enhanced Raman scattering”, Journal of Solid State Chemistry, Vol. 183, pp. 2968-2973.

Maezono, Takuya, Tokumura, Masahiro, Sekine, Makoto, Kawase, Yoshinori, (2011), “Hydroxyl radical concentration profile in photo-Fenton oxidation process: Generation and consumption of hydroxyl radicals during the discoloration of azo-dye Orange II”, Chemosphere, Vol. 82, pp. 1422-1430.

Mahmoodi, Niyaz Mohammad, (2011), “Photocatalytic ozonation of dyes using copper ferrite nanoparticle prepared by co-precipitation method”, Desalination, Vol. 279, pp. 332-337.

Mahmoudi, Morteza, Sant, Shilpa, Wang, Ben, Laurent, Sophie, Sen, Tapas, (2011), “Superparamagnetic iron oxide nanoparticles (SPIONs): Development, surface modification and applications in chemotherapy”, Advanced Drug Delivery Reviews, Vol. 63, pp. 24-46.

Oller, I., Malato, S., Sánchez-Pérez, J.A., (2011), “Combination of Advanced Oxidation Processes and biological treatments for wastewater

decontamination-A review", Science of the Total Environment, Vol. 409, pp. 4141-4166.

Matilainen, Anu, Gjessing, Egil T., Lahtinen, Tanja, Hed, Leif, Bhatnagar, Amit, Sillanpää, Mika, (2011), "An overview of the methods used in the characterisation of natural organic matter (NOM) in relation to drinking water treatment", Chemosphere, Vol. 83, pp. 1431-1442.

Nawrockia, Jacek and Kasprzyk-Hordern, Barbara, (2010), "The efficiency and mechanisms of catalytic ozonation", Applied Catalysis B: Environmental, Vol. 99, pp. 27-42.

Pradeep, T. and Anshup, (2009), "Noble metal nanoparticles for water purification: A critical", Thin Solid Films, Vol. 517, pp. 6441-6478.

Pocostales, P., Á lvarez, P., Beltrán, F.J., (2011), "Catalytic ozonation promoted by alumina-based catalysts for the removal of some pharmaceutical compounds from water", Chemical Engineering Journal, Vol. 168, pp. 1289-1295.

Roccaro, Paolo and Vagliasindi, Federico G.A., (2009), "Differential vs. absolute UV absorbance approaches in studying NOM reactivity in DBPs formation: Comparison and applicability", Water Research, Vol.43, pp.744-750.

Rosal, Roberto, Gonzalo, Maria S., Rodriguez, Antonio, Garcia-Calvo, Eloy, (2010), "Catalytic ozonation of fenofibric acid over alumina-supported manganese oxide", Journal of Hazardous Materials, Vol. 183, pp. 271-278.

Song, Wonho, Ravindran, Varadarajan, Koel, Bruce E., Pirbazari, Massoud, (2004), “Nanofiltration of natural organic matter with H_2O_2/UV pretreatment: fouling mitigation and membrane surface characterization”, Journal of Membrane Science, Vol. 241, pp. 143-160.

Staehelin, J. and Hoigné, J., (1985), “Decomposition of ozone in water in the presence of organic solutesacting as promotors and inhibitors of radical chain reactions”, Environ. Sci. Technol., 19, 1206–1213.

Sui, Minghao, Xing, Sichu, Sheng, Li, Huang, Shuhang, Guo, Hongguang, (2012), “Heterogeneous catalyticozonation of ciprofloxacin in water with carbon nanotube supported manganese oxides as catalyst”, Journal of Hazardous Materials, Vol. 227–228, pp. 227-236.

Van Geluwe, Steven, Braeken, Leen, Van der Bruggen, Bart, (2011), “Ozone oxidation for the alleviation of membrane fouling by natural organic matter: A review”, Water Research, Vol. 45, pp. 3551-3570.

Wang, Yan, Zhang, Hui, Chen, Lu, (2011), “Ultrasound enhanced catalytic ozonation of tetracycline in a rectangular air-lift reactor”, Catalysis Today, Vol. 175, pp. 283-292.

Wang, Zhenghua, Zhu, Shiyu, Zhao, Suping, Hu, Haibo, (2011), “Synthesis of core‐shell Fe_3O_4@SiO_2@MS (M= Pb, Zn, and Hg) microspheres and their application as photocatalysts”, Journal of Alloys and Compounds, Vol. 509, pp. 6893-6898.

Wei, Yan, Han, Bing, Hu, Xiaoyang, Lin, Yuanhua, Wang, Xinzhi, Deng, Xuliang, (2012), “Synthesis of Fe_3O_4 nanoparticles and their magnetic

properties", Procedia Engineering, Vol. 27, pp. 632-637.

Westerhoff, Paul, Aiken, George, Amy, Gary, Debroux, Jean, (1999), "Relationships between the structure of natural organic matter and its reactivity towards molecular ozone and hydroxyl radicals", Water Research, Vol. 33, pp. 2265-2276.

Ye, Bixiong, Wang, Wuyi, Yang, Linsheng, Wei, Jianrong, E, Xueli, (2009), "Factors influencing disinfection by-products formation in drinking water of six cities in China", Journal of Hazardous Materials, Vol. 171, pp. 147-152.

Zhao, Zhen-Ye, Gua, Ji-Dong, Li, Hai-Bo, Li, Xiao-Yan, Leung, Mei-Yee Kenneth, (2009), "Disinfection characteristics of the dissolved organic fractions at several stages of a conventional drinking water treatment", Journal of Hazardous Materials, Vol. 172, pp. 1093-1099.

Zularisama, A.W., Ahmada, Anwar, Sakinah, Mimi, Ismail, A.F., Matsuura, T., (2011), "Role of natural organic matter (NOM), colloidal particles, and solution chemistry on ultrafiltration performance", Separation and Purification Technology, Vol. 78, pp. 189-200.

呂理維，(2011)，"The assembly of magnetic metal ozone catalyst to decompose disinfection of by product"，東海大學環境科學與工程所碩士論文。

林嘉鈞，(2009)，"製備具標靶葉酸受體診斷及治療的多功能 pluronic 修飾四氧化三鐵"，國立高雄大學生物科技研究所碩士論文。

張勳鍊，(2010)，“Study of degradation of natural organic matters (NOMs) and reduction of disinfection by product (DBPs) in ozonation by design of experiment (DOE) and hydroxyl radicals”，東海大學環境科學與工程所碩士論文。

Appdenix

I. Particle size analysis

Intensity Distribution S/N : 127110

User	: Common	Group	: waterlab-particle	Repetition	: 1/1
Date	: 5/11/2012	File Name	: waterlab-particle_20120511_114946		
Time	: 11:49:46	Sample Information	: waterlab-particle		
SOP Name	: VISTA			Security	: No Security

Version 2.31 / 2.03

Intensity Distribution

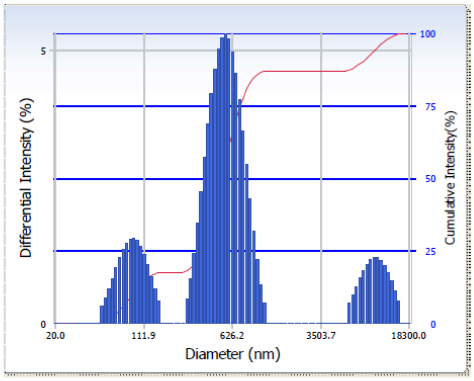

ACF

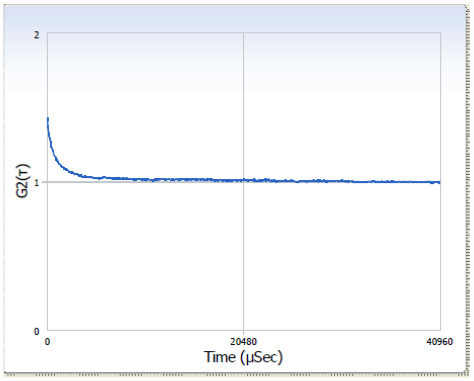

Distribution Results (Contin)

Peak	Diameter (nm)	Std. Dev.
1	90.5	24.4
2	571.2	188.5
3	10,261.2	2,566.3
4	0.0	0.0
5	0.0	0.0
Average	1,742.0	3,422.5

Residual : 1.511e-002 (O.K)

Cumulants Results

Diameter	(d)	: 973.4	(nm)
Polydispersity Index	(P.I.)	: 0.272	
Diffusion Const.	(D)	: 4.935e-009	(cm^2/sec)

Measurement Condition

Temperature	: 24.1	(°C)
Diluent Name	: WATER	
Refractive Index	: 1.3329	
Viscosity	: 0.9063	(cP)
Scattering Intensity	: 10397	(cps)

Intensity Distribution S/N : 127110

User	: Common	Group	: waterlab-particle-2	Repetition	: 1/1
Date	: 5/11/2012	File Name	: waterlab-particle-2_20120511_120856		
Time	: 12:08:56	Sample Information	: waterlab-particle-2		
SOP Name	: VISTA			Security	: No Security

Version 2.31 / 2.03

Intensity Distribution

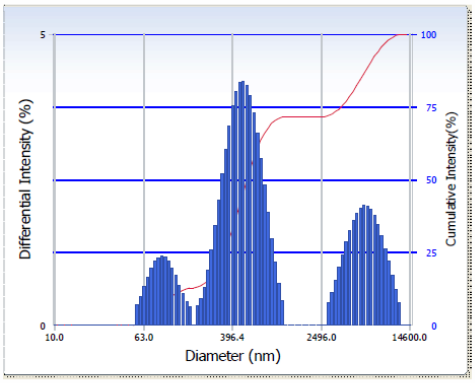

ACF

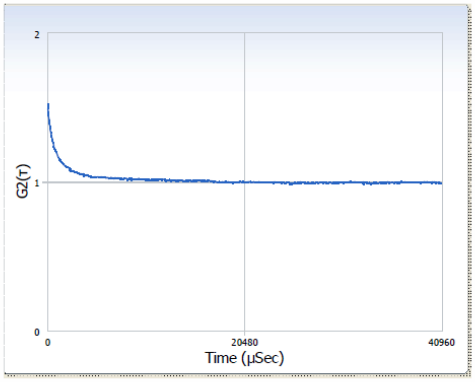

Distribution Results (Contin)

Peak	Diameter (nm)	Std. Dev.
1	96.5	27.2
2	515.6	194.3
3	6,482.1	2,287.9
4	0.0	0.0
5	0.0	0.0
Average	2,151.5	2,988.9

Residual : 3.044e-003 (O.K)

Cumulants Results

Diameter	(d)	: 709.6	(nm)
Polydispersity Index	(P.I.)	: 0.325	
Diffusion Const.	(D)	: 6.932e-009	(cm^2/sec)

Measurement Condition

Temperature	: 25.0	(°C)
Diluent Name	: WATER	
Refractive Index	: 1.3328	
Viscosity	: 0.8878	(cP)
Scattering Intensity	: 7196	(cps)

Intensity Distribution S/N : 127110

User	: Common	Group	: waterlab-particle-3	Repetition	: 1/1
Date	: 5/11/2012	File Name	: waterlab-particle-3_20120511_121727		
Time	: 12:17:27	Sample Information	: waterlab-particle-3		
SOP Name	: VISTA			Security	: No Security

Version 2.31 / 2.03

Intensity Distribution

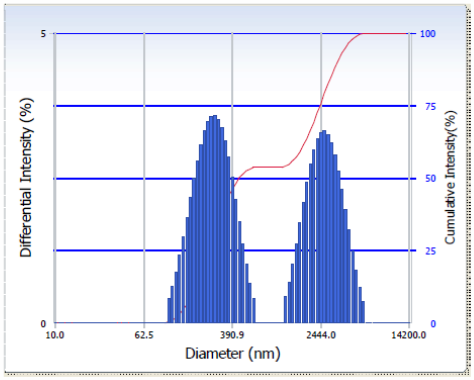

ACF

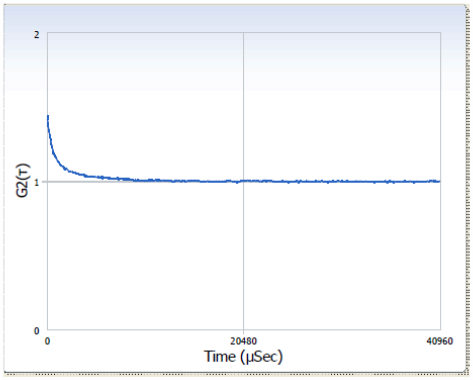

Distribution Results (Contin)

Peak	Diameter (nm)	Std. Dev.
1	277.5	109.4
2	2,780.6	1,027.0
3	0.0	0.0
4	0.0	0.0
5	0.0	0.0
Average	1,434.8	1,432.3

Residual : 2.932e-003 (O.K)

Cumulants Results

Diameter	(d)	: 677.6	(nm)
Polydispersity Index	(P.I.)	: 0.334	
Diffusion Const.	(D)	: 7.259e-009	(cm^2/sec)

Measurement Condition

Temperature	: 25.0	(°C)
Diluent Name	: WATER	
Refractive Index	: 1.3328	
Viscosity	: 0.8878	(cP)
Scattering Intensity	: 10624	(cps)

口試委員意見及回覆

陳谷泛 助理教授

---

1 意見: 摘要中英文需一致

回覆: 已在論文中摘要修正。

2 意見: 目的需放在第一章

回覆: 已在論文中第一章 (p. 3)修正

3 意見: Coumarin 去除率的表示方法

回覆: 已改為原始數據呈現(p. 53)

宋孟浩 副教授

---

1 意見: 補充合成催化劑之反應式

回覆: 已在論文中補充(p. 34)

2 意見: 補充催化劑之粒徑分析儀數據

回覆: 已在附錄中新增

3 意見: 催化劑之優勢需說明

回覆: 已在論文中補充(p.49)

馬英石 教授

1. 意見: 摘要需寫出結論

   回覆: 已在論文中摘要修正

2. 意見: 補充顆粒使用後之磁滯曲線

   回覆: 已於論文中 Fig. 4-5 補充 (p.46)

3. 意見: 為何不使用純相 Fe_3O_4?

   回覆: 純相 Fe_3O_4 粒徑分佈較寬，而且表面裸露，化學性質活潑，在空氣中極易氧化、易發生團聚現象，易使磁性材料失去單疇磁極、可分散性或者失去納米材料特有的性質。因此，為了改善 Fe_3O_4 磁性納米粒子的團聚現象，使其能很好的分散於載液之中，需要對其進行表面改性。

4. 意見: 腐殖酸礦化率為何偏低?

   回覆: 因為腐殖酸之成分比較複雜，且本研究所使用總有機碳分析儀是採用濕式氧化法，若將有機物改為結構較為簡單之化合物或改用高溫燃燒氧化法，可以明顯增進有機物的礦化率。